SILESIAN UNIVERSITY OF TECHNOLOGY
FACULTY OF ELECTRICAL ENGINEERING

Department of Power Electronics, Electrical Drives and Robotics

Master's thesis

To be determined

Student: **Igor Aleksander JANKIEWICZ**
Transcript no.: 285947

Type of studies: Extramural studies (MSc programme)
Field of study: Electrical Engineering
Programme: To be determined

Supervisor: PhD. EEng. Andrzej Latko

Gliwice 2020

CONTENTS

1 INTRODUCTION

This Master's thesis is focused on Piezoelectic Energy Harvesting in general. Apart from the explanation of the actual energy scavenging process, it also covers a design of a proper data acquisition system used for evaluation and development of piezoelectric-based generators.

1.1 Motivation

Nowadays, electrical energy itself is taken for granted by most of the people. It may be a result of the fact that most of household appliances and daily use items require that energy to operate. Moreover, almost any of our tasks requite a proper illumination, Internet access or simply the outlet to liven any tool we might need at the moment. To conclude, it is almost impossible to imagine our life without an access to the power gird.

On the other hand, it is important to keep in mind that most of electricity we utilize comes from non-renewable fuels such as coal, liquid gas or crude oil. At some point, humankind is to face a problem of insufficient deposits of these materials, therefore it tremendously important to look for alternatives. Of course, people have already taken advantage of water, wind or solar radiation, what is proven by the existence of many green power plants around the world. Unfortunately, one of the major problems faced by all of there plans is the intermittent access to the energy source. Moreover, there are many places that does not allow to use any of these well explored solutions, forcing engineers to look for new ones. This could be a reason why vibrational energy is getting more awareness over last years.

Energy harvesting from vibration gives many new possibilities, especially in IoT (Internet of Things) applications, as well as in industrial environment. The second application seems particularly tempting, as in many industrial applications, there is a lot of vibration involved, what gives a wide scope for custom sensor development. Piezoelectric harvesters are relatively compact, therefore it is possible to install them in inaccessible places. Moreover, they are robust, providing that a proper enclosure is used for mechanical protection.

All of mentioned factors gained author's interest, and in the event prompted to work on this subject within the confines of this thesis.

1.2 Objective of a Master's thesis

The main goal stated by the author is to examine a potential of vibration-based energy scavenging. In order to do so, number of different aspects need a thorough investigation. Undeniably, much of the focus would be put on the energy harvester itself. Nevertheless, a proper measurement and data acquisition system is also an important aspect throughout the entire work, since it will allow confirm or deny thesis statements posed during the research. In addition, the design process of the mentioned device would allow a more in-depth analysis of the piezoelectric generator itself, since the understanding of its operation is the only way to come up with a suitable measurement system.

Returning to the piezoelectric generator, the first thing to look at is the theory behind the piezoelectric effect. Then, there would be a description of the piezoelectric cantilever and its properties. Subsequently, the complete mechanical and electrical model would be studied.

Once the required theory is introduced, it is possible to focus exactly on the topic.

2 CONCEPT OF ENERGY HARVESTING

Energy Harvesting is a process of using ambient energy by converting it into a usable form, i.e. electricity or heat. It is important to point out that energy harvesting has been around for quite a long time, since solar panels, wind turbines and water turbines are in constant use for a few decades, providing people with environmentally clean energy [1].

There are some important issues related to any energy source that could be potentially used for harvesting. First of all, it is crucial to evaluate intensity and availability of that source. Subsequently, one should find out a cost-effectiveness of the solution as well as the influence of the harvesting process on the primary energy source [1].

Vibration-based Energy Harvesting incorporates a number of different fields of study, i.e. material science, mechanics or electrical engineering, just to name a few. Last sentence implies that the analysis of a piezoelectric generator itself is not a straightforward process. The electromechanical response of this device relies thoroughly on the source of ambient energy [2].

The concept of piezoelectric energy harvesting is strongly related to the improvement of electronics manufacturing technologies. Due to fact that most of devices are becoming more energy efficient, it allows to seek for potentially useful energy in solutions that have been neglected before. This perfectly applies to vibrational energy [3].

2.1 Piezoelectric materials

Certain solid materials (ceramics or crystals) lacking inversion symmetry exhibits charge generation phenomena when an external force is applied to it. This phenomenon is called the piezoelectric effect and it was invented and firstly introduced by the brothers Pierre and Jacques Curie in 1880 [4].

Putting it simply, when a piezoelectric material is squeezed, an electric charge is collected in its surface. Conversely, the voltage drop across the piezoelectric material generates mechanical deformation. Piezoelectricity is related to a non-uniform charge distribution within crystal's unit cells. Due to deformation, positive and negative charges displace, generating an electric potential in the crystal, even though the overall the crystal itself remains electrically neutral [2].

2.1.1 Mathematical description of the piezoelectric effect

Describing properties of piezoelectric materials is not a straightforward task, especially when trying to provide only basic information regarding this topic. For mechanical problems, it is a common practise to use so-called constitutive equations to describe material's response to applied force. This approach can also be used for solving electrical problems [5].

Owing to the fact that piezoelectric materials are concerned with both mechanical and electrical properties, these must be considered simultaneously. By combining these areas together the so-called piezoelectric constitutive equations are introduced.

The most common mechanical constitutive equation is known as Hooke's Law -see Equation 2.1 [5]. Please note that underlined symbols stand for vectors.

$$\underline{S} = \underline{s}^E \cdot \underline{T} \tag{2.1}$$

where:

$\underline{S}$ – Mechanical Strain,
$\underline{s}^E$ – Stiffness or Compliance under zero or constant electrical field,
$\underline{T}$ – Mechanical Stress

Since the electrical properties also need to be taken into account, a so-called dielectrics equation is introduced [4].

$$\underline{D} = \underline{\varepsilon}^T \cdot \underline{E} \tag{2.2}$$

where:

$\underline{D}$ – Charge Density or Electrical Displacement,
$\underline{\varepsilon}^T$ – Dielectric Permittivity under zero or constant stress,
$\underline{E}$ – Electrical Field

Both of above-mentioned constitutive equations are now combined to create one coupled equation. This way, providing that mechanical properties of the piezoelectric material are known, it is possible to describe or model the harvester [5]. One should note the addition of coupling terms ($\underline{d}^t \cdot \underline{E}$ and $\underline{d} \cdot \underline{T}$) required for the proper analysis.

$$\begin{aligned} \underline{S} &= \underline{s}^E \cdot \underline{T} + \underline{d}^t \cdot \underline{E} \\ \underline{D} &= \underline{d} \cdot \underline{T} + \underline{\varepsilon}^T \cdot \underline{E} \end{aligned} \tag{2.3}$$

where:

$\underline{d}$ – Matrix for the direct and reversed piezoelectric effect,
$\underline{d}^t$ – Transposed Matrix for the direct and reversed piezoelectric effect

By taking Equation 2.3 into consideration, it is possible to come up with the detailed matrix notation for a standard PZT crystal, very similar to those used for energy harvesters - see Equation 2.4 [4].

$$\begin{aligned} \begin{bmatrix} S_1 \\ S_2 \\ S_3 \\ S_4 \\ S_5 \\ S_6 \end{bmatrix} &= \begin{bmatrix} s_{11}^E & s_{12}^E & s_{13}^E & 0 & 0 & 0 \\ s_{12}^E & s_{11}^E & s_{13}^E & 0 & 0 & 0 \\ s_{13}^E & s_{13}^E & s_{33}^E & 0 & 0 & 0 \\ 0 & 0 & 0 & s_{44}^E & 0 & 0 \\ 0 & 0 & 0 & 0 & s_{44}^E & 0 \\ 0 & 0 & 0 & 0 & 0 & 2(s_{11}^E - s_{12}^E) \end{bmatrix} \cdot \begin{bmatrix} T_1 \\ T_2 \\ T_3 \\ T_4 \\ T_5 \\ T_6 \end{bmatrix} + \begin{bmatrix} 0 & 0 & d_{31} \\ 0 & 0 & d_{31} \\ 0 & 0 & d_{33} \\ 0 & d_{15} & 0 \\ d_{15} & 0 & 0 \\ 0 & 0 & 0 \end{bmatrix} \cdot \begin{bmatrix} E_1 \\ E_2 \\ E_3 \end{bmatrix} \\ \begin{bmatrix} D_1 \\ D_2 \\ D_3 \end{bmatrix} &= \begin{bmatrix} 0 & 0 & 0 & 0 & d_{15} & 0 \\ 0 & 0 & 0 & d_{15} & 0 & 0 \\ d_{31} & d_{31} & d_{33} & 0 & 0 & 0 \end{bmatrix} \cdot \begin{bmatrix} T_1 \\ T_2 \\ T_3 \\ T_4 \\ T_5 \\ T_6 \end{bmatrix} + \begin{bmatrix} \varepsilon_{11}^T & 0 & 0 \\ 0 & \varepsilon_{11}^T & 0 \\ 0 & 0 & \varepsilon_{33}^T \end{bmatrix} \cdot \begin{bmatrix} E_1 \\ E_2 \\ E_3 \end{bmatrix} \end{aligned} \tag{2.4}$$

Please note that the subscripts 1, 2, 3 stand for the x, y and z axis, respectively. Due to the fact that strain and stress tensors are symmetrical, it possible to re-label subscripts using the Voigt notation. having said that, the subscripts look as follows: 11 $\rightarrow$ 1, 22 $\rightarrow$ 2, 33 $\rightarrow$ 3, 23 $\rightarrow$ 4, 13 $\rightarrow$ 5 and 12 $\rightarrow$ 6 [4]. First three subscripts are related to forces applied perpendicular to cartesian coordinate system axes. The rest of them describe shear forces. This notation convention simplifies the matrix description of the piezoelectric structures. Once again, it is vital to highlight that the presented mathematical description of the piezoelectricity phenomena is by all means very superficial.

The coupling factor d shows three possible modes applicable to piezoelectric beams related to its operation. Please not that d_{15} is associated with the shear stress, therefore only d_{31} and d_{33}

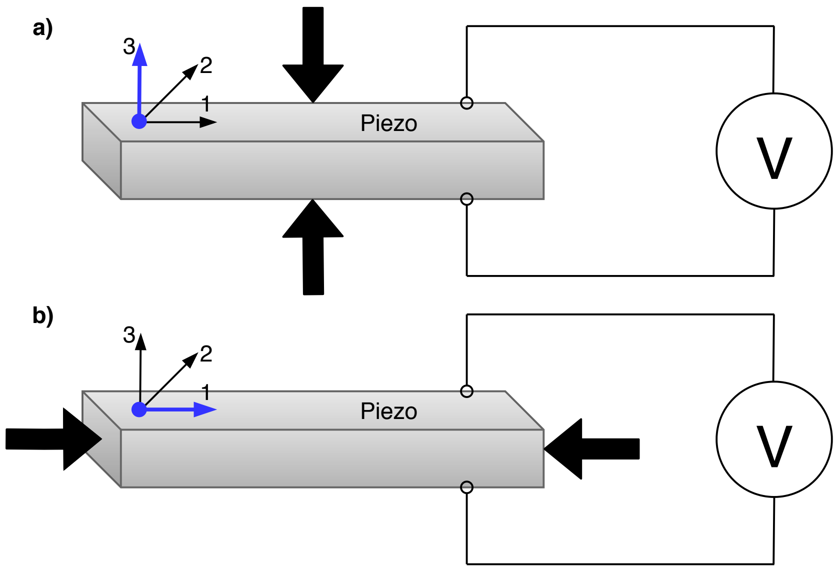

Figure 2.1: Operation modes of the piezoelectric element a) d_{33}, b) d_{31}

modes are to be taken info further consideration. For visualisation purposes, one should look at the Figure 2.1.

In the first presented mode (d_{33}), the stress acts in the same direction as the voltage appears - in both cases along the z axis. When it comes to bending action, this mode is not the best description of what is happening in the crystal. Significantly better description is provided by d_{31} mode, where the stress is applied to the x axis and the voltage is induced in the z axis [4]. Bending process forces the beam to stretch and compress, what yields some potential across the electrodes.

2.1.2 Most popular piezoelectric materials for harvesting applications

Currently, the most popular material utilized in harvesters is so called PZT (lead zirconate titanate). It was developed at the Tokyo Institute of Technology in the 1950s [2]. Nowadays, it can be found in a few different flavours, what would be described more precisely later. This material is a polymer composite, which is very brittle and prone to crack when overstressed [4].

As described in the previous paragraph, PZT has a number of different types that vary with electrical and electromechanical properties. The simplest division includes hard and soft types - PZH-5H and PZH-5A, respectively. Soft piezoceramics are more susceptible to changes caused by the stress. This is one of the aspects why PZH-5H is the most common choice for piezoelectric equipment. On the other hand, one of the biggest manufacturers of harvesters [6] is mentioning that PZH-5A is more temperature stable. Nevertheless, PZH-5H remains the best choice in terms of performance versus price.

2.1.3 Properties of piezoelectric materials

Properties of piezoelectic materials strongly depend on the direction of the stres and orientation of the polarization [1]. It is characterized by the constants listed in the Table

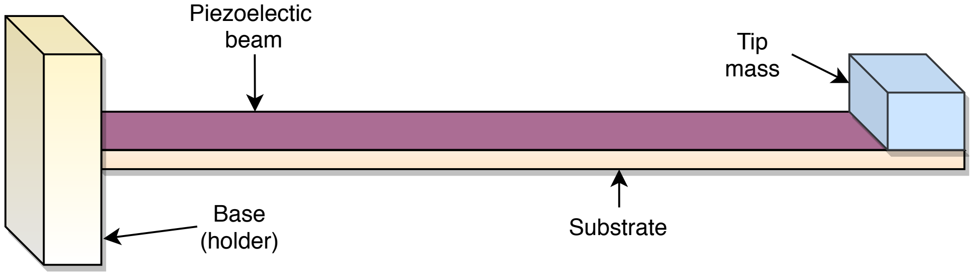

2.2 Efficiency and power density

Piezoelectric generator is truly a non-linear device. It produces maximum output power at its resonance frequency, which depends on a number of factors.

Power density of the harvesters is expressed as the output power divided by the device volume for the given input [2]. In case of vibrational energy, the input is the acceleration level and the frequency. An output of the piezoelectric generator provides voltage levels suitable for many electronics systems, therefore it is often unnecessary to add additional power electronics, what has an influence on efficiency.

Table 2.1: Common data for some of Energy Harvesting Sources [1]

Type	Conditions	Power Density	Area or Volume	Energy/Day
Vibration	$1m/s^2$	$100\mu W/cm^3$	$1cm^2$	$8.64J$ (continuous vibration)
Solar	Outdoors	$7500\mu W/cm^2$	$1cm^2$	$324J$ (sunny half a day)
Solar	Indoors	$100\mu W/cm^2$	$1cm^2$	$4.32J$ (sunny half a day)
Thermal	$\Delta T = 5°C$	$60\mu W/cm^2$	$1cm^2$	$2.59J$ (heat available for half a day)

2.3 Clamping

Effective clamping is really important for piezoelectric beams. In order to achieve best performance, it is crucial to provide proper holder that gives reliable operation regardless of vibration level - see Figure 2.2.

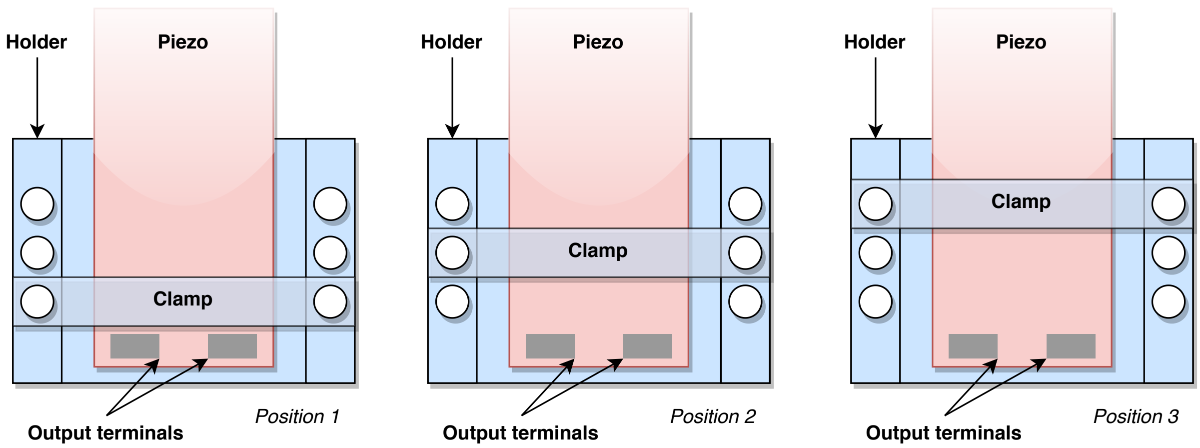

Figure 2.2: Clamping problem explanation

For the sake of this project, the holder provided by the manufacturer would be used for evaluation purposes. The clamp bar is going to hold the beam in place with help of bolts and washers.

According to the manufacturer's datasheet [6], the second position of the clamp is a default configuration for all products. The third position of the clamp comes in handy when one need to increase the resonant frequency of the piezo wafer. On the other hand, the first position reduces the resonant frequency. It is noted that this hardware configuration is not recommended for energy harvesting applications due to stiffness issues.

2.4 *Tip mass*

Piezoelectric energy harvesters are frequency-dependent devices. In order to achieve their maximum efficiency, it is necessary to operate close to its resonant frequency. Piezoelectric beams may need some tuning procedures in order to match the frequency of the vibrating source, thus allowing to ensure most energy efficient harvesting.

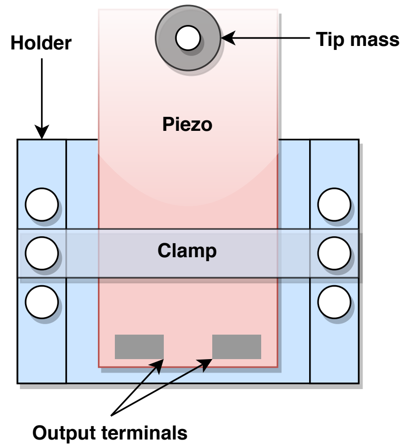

Figure 2.3: Tip mass illustration

As mentioned in the previous subsection, frequency tuning may be performed by changing the clamp position. Unfortunately, this option does not allow for precise trimming, therefore additional techniques are often required. One of the most popular ones incorporated the tip mass attached at the end of the piezoelectric wafer. Providing that the operating frequency is fixed and known, it is possible to determine the exact tip mass required to tune the beam.

In this case, m is the effective mass, m_k is the added tip mass, k is the effective stiffness and f is the natural frequency. One should take into account that these equations are valid only when the applied tip mass is centered and places according the the manufacturer's guidelines.

$$f = \frac{\sqrt{\frac{k}{m+m_t}}}{2 \cdot \pi} \tag{2.5}$$

$$m_t = \frac{k}{(2 \cdot \pi \cdot f)^2} - m \tag{2.6}$$

It is important to note that the natural frequency of the piezoelectric material is affected by such factors as temperature, manufacturing process, clamping conditions as well as vibration amplitude [6]. Moreover, the resonance frequency is highly affected by the load powered by the harvester.

2.5 Piezo beam resonance conditions

To determine the natural frequency of the beam, one should apply a mechanical impulse to the beam and monitor its response. In order to do so, it is handy to use an oscilloscope in order to monitor the output of the loaded piezoelectric beam. The frequency of the decaying wave is equal to the natural frequency of the beam [6].

3 MEASUREMENT SETUP DESIGN

A proper measurement process is a crucial part of this project. Having said that, a custom data acquisition board is to be designed.

First of all, it is vital to highlight most important features required to achieve desired performance. There are four major aspects that have to be taken into account, namely, the ADC resolution as well as the input voltage range, the bandwidth and high input impedance of the analog front-end. Apart from that, one should take care of easy interfacing to personal computer, thus compact size and USB interface would be considered as huge assets.

The previous paragraph introduced briefly main functionalities of the target device. It is quite easy to notice that there would be a lot of trade-offs to consider through the design process. Compact size and the complex analog circuitry usually do not mix, especially when planning to get a device of USB mass storage size. These facts are forcing the designer to look for a microcontroller that provides decent ADCs, also in terms of the sampling rate. Since the project is dealing with piezoelectric generators, there is always a risk of relatively high voltages at the input terminals, especially when harvesters are not connected to any load. To face this problem, the data acquisition board would be equipped with two different means of protection. The first one takes care of the input stage of the device. The second one is a classic galvanic isolation between the microcontroller (as well as the analog front end) and the personal computer. This way, there is no risk of damaging host devices utilizing the data acquisition system. The summary of the above-mentioned description is presented in the Figure 3.1.

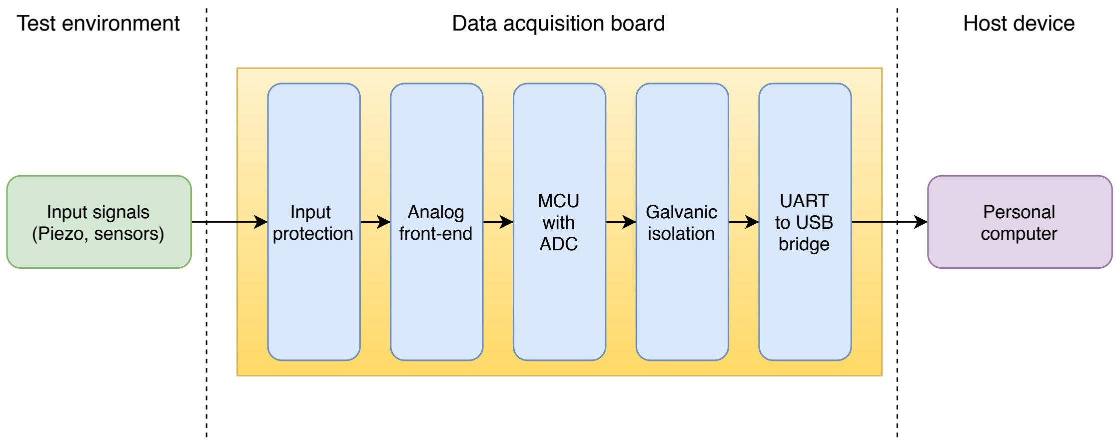

Figure 3.1: Measurement setup overview

3.1 Design requirements

The first step of the design process is to determine desired input ratings as well as data acquisition capabilities. The piezoelectric device used in this project would be the major signal source during all experiments. Its datasheet [6] does not state any fixed maximum ratings.

Instead, it provides exemplary results obtained by varying acceleration amplitude, frequency, tip mass and load resistance - see Table 3.1.

Table 3.1: Exemplary piezoelectric harvester response. Data from PPA-1001 datasheet [6]

Acceler. ampl. (g)	**Freq.** (Hz)	**Tip mass** $(gram)$	**RMS power** (mW)	**RMS voltage** (V)	**RMS current** (mA)	**Load** $(k\Omega)$
0.25	132	0.0	0.1	1.1	0.1	17.9
0.50	131	0.0	0.2	1.9	0.1	18.3
1.00	131	0.0	0.7	3.4	0.2	15.7
2.00	129	0.0	2.2	5.4	0.4	13.0
0.25	60	1.9	0.1	2.9	0.0	61.0
0.50	60	1.8	0.5	3.3	0.2	20.8
1.00	60	1.7	1.8	7.1	0.3	28.6
0.25	22	22.8	1.4	9.0	0.1	60.4
0.50	22	22.8	4.4	17.3	0.3	67.6

As mentioned in the previous paragraph, there is no constrained area in terms of vibration frequency and level stated by the manufacturer. Based on the data presented in the Table 3.1, the designer is relatively free to determine the operating frequency range as well as input signal range recorded at at the harvester's output. When considering bandwidth and sampling rate, it is important to take into account the Nyquist criterion. It states that the sampling rate has to be twice the highest frequency in the signal [7]. Assuming maximum vibration frequency of 500Hz, more than 1000 samples per second need to be captured.

Of course, this sampling rate only allows to reproduce an incoming signal (sinusoidal wave) as a corrupted triangle, since there is not enough data points to accurately reflect the sine shape. To solve this problem, the sampling rate should be increased by factor of 5 or so, what ultimately yields at least 5000 samples per second (sps). To illustrate the problem, Figure 3.2 is introduced. It can be easily seen that sampling rate as high as twice the input signal frequency is definitely not enough. Having said that, the minimum expected sampling rate is to be at least 5000 sps.

It is likely that the microcontroller used in the data logger would use some kind of a serial communication protocol. Assuming that more than one signal is recorded at the time and the baud rate is fixed at the same level, the maximum input signal frequency would be divided by the number of active channels. For example, for 2 channel measurement, the maximum input signal frequency is 250Hz and so on.

One of the previous paragraphs mentioned the piezoelectric harvester as the main input signal source. Knowing that the device produces a sinusoidal output, the analog front-end has to be able to capture AC signals, preferably of a relatively high amplitude. This requirements force the designer to develop symmetrical power supply for the input section as well as the circuitry allowing to add offset to the signal before it reaches the ADC input. A reason is that the ADC of the microcontroller is likely to accept only unipolar signals within tightly specified range. Remaining channels would be able to interface DC signals only, what makes them suitable for external sensors such as the accelerometer.

When considering the maximum input signal level, one has to note that it should not exceed supply voltage of operational amplifier used in the input section. In case of the designed device, the power supply would be industrial $\pm 15VDC$, as it helps to maintain compatibility with wide range of available operational amplifiers. Based on the last sentence, the maximum input voltage is specified to $\pm 15V$ for the AC input and $+15V$ for DC inputs. In order to assure proper operating conditions for the analog-front end, an additional input protection is to be

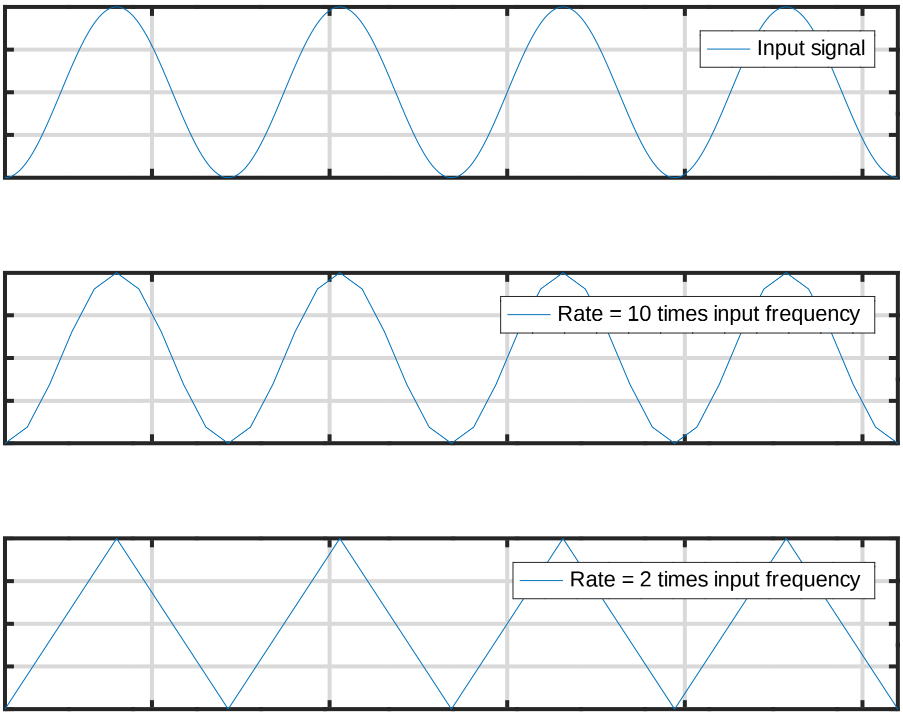

Figure 3.2: Captured waveform versus sampling rate

provided.

There are two last aspect that need some care. The first one is the resolution of the ADC that would be used to capture the incoming signal. The second one is the input impedance of input channels.

As to the first point, it is useful to have a look at technical details of commonly available oscilloscopes, since they can be treated as a nice reference. Most of them utilize 8 or 10-bit ADCs, mostly because of bandwidth requirements as well as the sampling time. In case of this design, the bandwidth is significantly reduced, what allows to look for a bit more resolution, of course still bearing in mind that all the processes are handled by one modest microcontroller. Putting it all together, an 14-bit ADC is going to be a desired data converter.

The last point relates to the impedance of analog inputs. Piezoelectric harvesters are high output impedance devices [1], therefore it is desirable to maintain as high input impedance of the analog front-end as possible, in order not to disturb the incoming signal. There are two potential problems that may occur when designing the input stage. As it can be guessed, the input signal has to be divided before it gets to the analog-to-digital converter. The easiest way to go is to put a voltage divider directly at the output of the harvester. Unfortunately, this circuit would have a significant influence on the impedance seen from piezo generator's output terminals, thus posing a risk of changing its operating conditions. To deal with this problem, the incoming signal is to be buffered before any further processing. This is where low input bias current operational amplifiers would come in handy. The second risk is related to the protection circuitry attached to input terminals. Once the input signal gets to high, it would be clamped in order to protect the data acquisition board. Unhappily, it would also disturb the measured object due to rapid change of the impedance seen at mentioned harvester's output terminals. The only way to deal with this issue is to provide relatively high supply voltage for buffering amplifiers and adjust the load as to meet the input voltage requirements.

As a summary of design considerations included in this subsection, Table 3.2 has been created.

Table 3.2: Summary of requirements for the data acquisition board

Requirement	Value
Max. input signal frequency (Sine)	500Hz
Min. sampling rate	5000sps
Min. ADC resolution	14-bit
Max. input voltage range (p-p)	15V
Input impeadnce	TBD

3.2 Accelerometer board

As it has been previously mentioned, is is necessary to constantly monitor vibration level during all the experiments. These measurements will be a reference for the results obtained using the piezoelectric harvester, as they easily allow to correlate generated power and current vibration level.

The piezoelectric beam used throughout the research is mounted in a 3D-printed holder provided by the device manufacturer. Apart from a proper fit, it allows to attach some external electronics by means using nice mounting holes. It is worth to take advantage of this feature, therefore designed electronics would be compatible with the handler.

3.2.1 Most important parameters of the accelerometer

As to the electrical and electromechanical properties of the accelerometer, there are a few aspects that should be highlighted. The first one is the measurement range. By checking the maximum acceleration of the beam, it is possible to estimate required range for the sought integrated circuit. Next, the frequency response and output signal type need to be determined. Frequency response describes the measurement resolution that could be understand as the smallest detectable acceleration [8]. By mentioning the type of the output signal, it was intended to distinguish between analog and digital output types. It is planned to synchronize the accelerometer output with the piezoelectric cantilever response, so the analog output is more suitable and easier to use.

Harvester's datasheet [6] does not mention the exact upper limit of allowed vibration level. According to the Table 3.1, the maximum acceleration amplitude mentioned by the manufacturer is 2g. Without any additional information, it is reasonable to treat this value as the upper acceleration limit. The same applies to the frequency response, which is also not described precisely. Again, Table 3.1 states the maximum operation frequency at the level of 132Hz. In this case, the minimum acceptable bandwidth of the accelerometer would be roughly 200Hz. As it was mentioned in the previous paragraph, it is intended to use the analog output accelerometer. A summary of the above-mentioned choices is presented in the Table 3.3.

3.2.2 Selection of the integrated circuit

After a thorough market research, a proper device has been found - see Table 3.4. Apart from parameters listed in the table, the selected accelerometer has the following features: small

Table 3.3: Summary of requirements for the accelerometer

Requirement	**Value**
Max. acceleration value	$\pm 2g$
Max. operating frequency	300Hz
Output type	Analog

SMD package, 3.3V supply operation, low power consumption and tunable bandwidth filters for every axis. Moreover, it exhibits non-linearity at a level of 0.3% [9].

Table 3.4: Parameters of the selected parameter - taken from the datasheet [9]

Parameter	**Value**
Model	ADXL335
Manufacturer	Analog devices
Output type	Analog
Max. acceleration value	$\pm 3g$
Bandwidth	up to 1600Hz

As it can be seen, the above-mentioned device fulfils the requirements presented in the previous subsection. At this point, it is necessary to think about additional circuitry allowing to take advantage of the selected integrated circuit. In order to do so, a small PCB is to be designed.

3.2.3 Accelerometer board design

The accelerometer board should be a battery powered device, as it is going to be used throughout tests in different types of environment, many times without an access to any power supply. Moreover, battery operation allows for a better performance in terms of noise generated on supply rails. Additionally, the board is ought to be equipped with a temperature sensor, in case some tests are to be performed in extreme temperatures and the exact temperature value is needed to know.

Figure 3.3 presents the diagram of designed board. It can be divided into two main parts, namely a power supply with a battery charger and a sensing part including the accelerometer and the temperature sensor.

As to the power supply part, for the convenience, the entire board in powered using a micro USB port, which is fused for safety purposes. Right after the input, there is a single cell battery charger (BRCL4054CME by Blue Rocket Electronics [10]). Charging current is set using just one resistor. Moreover, it incorporates such function as C/10 charge termination, a soft-start feature as well as an open-drain output used for signalling purposes.

Power storage is maintained by means of a 110mAh lithium-polymer battery (LIPO511422 by MAXPOWER). It is equipped with a complete protection circuitry, so it is unnecessary to include additional protection on the accelerometer board. The battery manufacturer claims the cycle life of 1000 cycles.

Right after the ON/OFF switch, there is a low dropout linear regulator supplying the rest of circuits (AP2112K-3.3TRG1 by Diodes Incorporated [11]). It is a 600mA output, low noise regulator with $\pm 1\%$ output voltage accuracy.

One of the sensors placed on this board is the accelerometer mentioned in the previous section. The second one is a low-power linear temperature sensor (MCP9700T-E/TT by Microchip

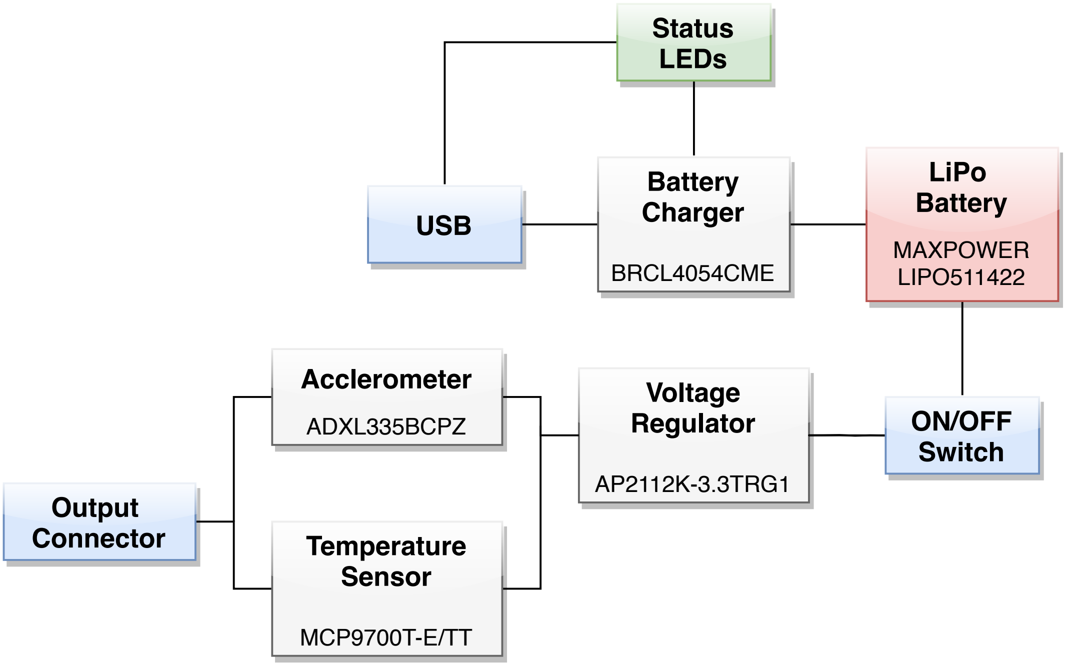

Figure 3.3: Accelerometer board diagram

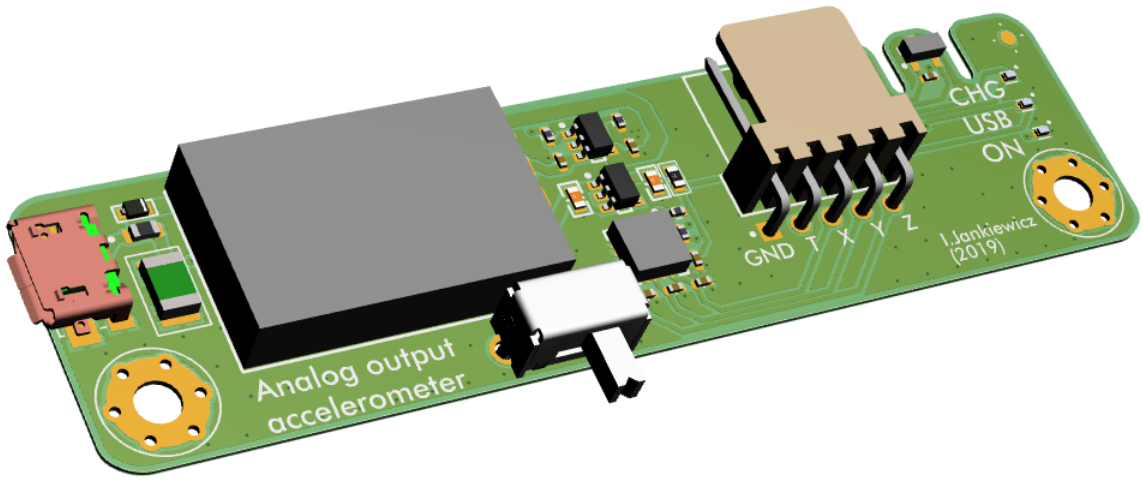

Figure 3.4: Accelerometer board top side view

[12]). Since the linear output is one of the requirements for all sensors used in this project, this kind of device was an easy choice. MCP9700 includes circuitry converting temperature to voltage and provides accuracy of $\pm 2°C$, which is by all means acceptable for this application.

Figures 3.4 and 3.5 present the final design. As it can be seen, a relatively compact and intuitive device has been developed. A standard connector with 2.54mm pitch is used to allow easy access to the board. There are two reinforced holes for mounting screws. The bottom side of the PCB includes large past allowing to solder cables connected to piezoelectric beam terminals in order to make the construction more robust.

This board is going to be an inherent part of most experiments performed throughout this thesis.

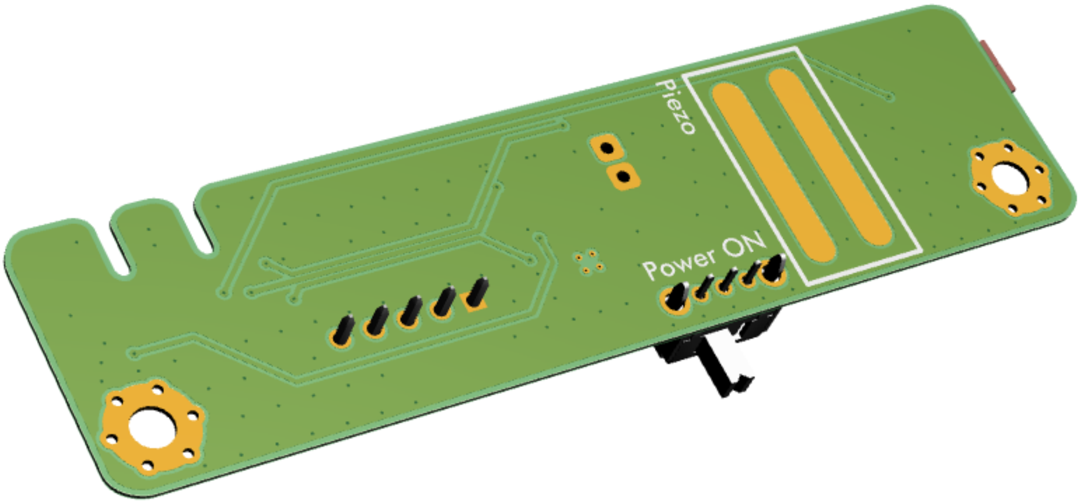

Figure 3.5: Accelerometer board bottom side view

3.3 *Data acquisition board design*

3.3.1 *AC input section*

The data acquisition board is going to be equipped with one AC-tolerant input channel. Additionally, there would be three different AC inputs connected to the AC channel by means of relays, what would allow easy selection of input source. The AC channel would be handy when piezoelectric beam is loaded with a resistive load only (excluding a rectifier). In order not to damage the microprocessor and other circuitry that is powered from a single supply, some signal conditioning is required.

3.3.1.1 Input protection

An important aspect (often overlooked though) is proper input protection for analog circuitry. At this point it is important to highlight that signal conditioning would be based on a variety of different operational amplifier-based circuits. Having said that, one should consider problems related to these devices as well as the influence of protection circuit on measurement results.

One of most popular means of protection for op-amps are clamping diodes along with current limiting resistors. Nowadays, popular operational amplifiers incorporate ESD protection diodes into their input circuitry, which is surely very helpful in most cases, nevertheless it can be a source of potential problems. These diodes are clamped to supply rails in order to provide return path for currents generated by ESD-related events. These happen once the input voltage gets higher than supply rail voltage plus voltage drop (usually around 0.7V) or lower than negative rail voltage minus the diode voltage drop, respectively [13]. In normal conditions these diodes remain transparent.

It is important to remember that the clamping circuit is going to have an influence on measurement results if designed improperly. Now, it is time to recall a very important parameter related to inputs of the operational amplifier, namely the Input Bias Current I_{bias}, which is inherently related to any ”real” (and non-ideal) Op Amp. It’s value is going to have a direct influence on the clamping circuit design, what would be explained in a more detailed manner soon.

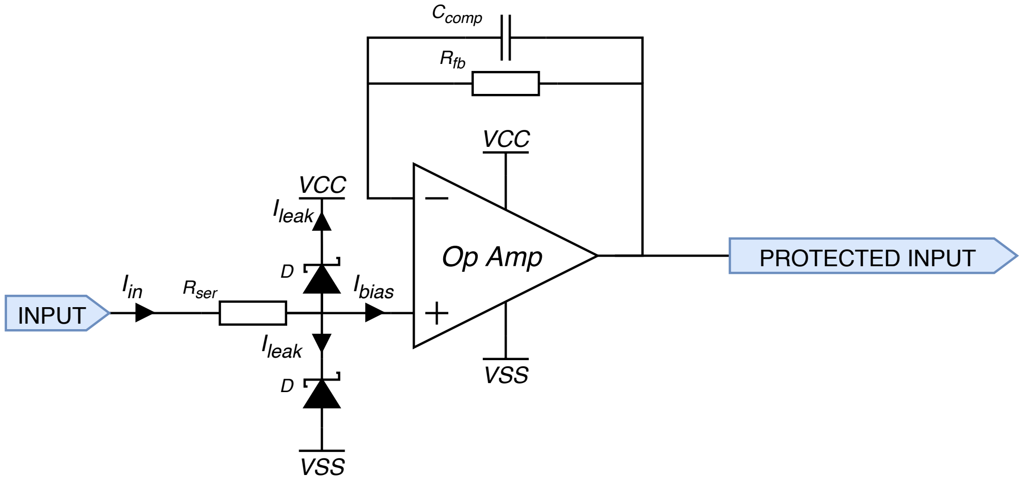

Figure 3.6: Clamping overvoltage protection scheme

The Input Bias Current I_{bias} is a DC current required by the Op Amp's inputs to establish proper biasing of input stage transistors [14]. It ranges from a few picoamps to a few microamps. This current is going to flow through the series protection resistor, generating a voltage drop proportional to mentioned current value multiplied by the series resistance. The explanation is presented in the Figure 3.6.

Another unwanted, but also unavoidable error source is the Reverse Leakage Current I_{leak} of clamping diodes, which depends on the value of reverse voltage applied to its terminals. All unwanted currents add up and flow through the series protection resistor R_{ser} generating the voltage drop. The total error voltage V_{error} is equal to the mentioned voltage drop multiplied by the gain of the operational amplifier A_u - see Equation 3.1.

$$V_{error} = (R_{ser} \cdot (I_{bias} + I_{leak1} + I_{leak2})) \cdot A_u \tag{3.1}$$

Of course, apart from the error generation, the clamping circuit plays a crucial role in operational amplifier's inputs protection, since it allow to deal with excessive voltage without any problems. The maximum continuous input voltage can be calculated if the value of series resistance, the Forward Continuous Current I_f, op-amp supply voltage V_{cc} and the diode forward voltage drop V_{fd} are known. Peak input voltages can even be even higher, as this parameter depends strongly on the current value flowing through the protection diode.

$$V_{in(MAX)} = V_{cc} + R_{ser} \cdot I_f + V_{fd} \tag{3.2}$$

To summarize, it is vital to emphasize once again the importance of the champing circuit. Even though it can introduce some error, careful component selection allows to find the balance between the performance and protection properties. It is important to use Schottky diodes, as only low voltage drop devices ale able to bypass the internal ESD protection diodes placed at inputs of the op-amp, what ultimately prevents from unintended damage of the protected device.

Taking into account all information included in this paragraph, a proper clamping diode has been chosen. Its parameters are presented in the Table 3.5.

3.3.1.2 Buffering

This project is all about high impedance signals, what automatically forces designer to make the analog front-end ”invisible” for the signal source. In order to do so, the input stage of

Table 3.5: Parameters of the selected parameter - taken from the datasheet [15]

Parameter	Value
Model	BAS40-02V-V-G
Manufacturer	Vishay Semiconductors
Type	Schottky
Package	SOD-523
Repetitive peak reverse voltage V_{RRM}	40V
Forward continuous current I_F	120mA
Leakage current I_R	20nA (Typ.)
Forward voltage V_F	380mV (I_F=1mA)

the data acquisition board is supposed to draw as little current as possible.

The design requirements states the maximum peak-to-peak input voltage as high as 12V. This fact obliges to supply operational amplifiers using at least industry's standard ±15V rails, providing that op-amps used in the project would not get saturated. Rail-to-rail devices may be helpful in this situation.

Figure 3.6 presents the exact configuration of the op-amp circuit. It is called a voltage follower or a buffer. At this point, it is very important to once again look at the estimated current consumption of the input stage. Previous paragraph stated all unwanted current paths that deteriorate the performance of the entire circuit. The leakage current I_{leak} of diodes should be kept as low as possible (in order of nanoamperes). The another error source highlighted before is the input bias current I_{bias} of the operational amplifier's non-inverting input. Since the buffer circuit is used, the input impedance of the amplifier is limited by the I_{bias} only. Modern op-amps can draw as little bias current as a few picoamperes, therefore, the impact of this device is negligible providing that the proper integrated circuit will be used.

When designing op-amp circuits, it is important to match the impedance of both inputs in order to avoid output voltage offsets. In case when these impedances are not equal, offset voltages generated by the bias current of both inputs have no chance to cancel out, introducing another error source [14]. The compensating capacitor C_{comp} used in the feedback network (along with the feedback resistor R_{fb}) is forming an RC filter slowing down the amplifier's response and making it more stable, but it is necessary to keep its resonant frequency at reasonable level in order not to disturb the input signal.

After a market research, the appropriate operational amplifier has been found - see Table 3.6. At this point is possible to calculate the error voltage introduced by the input protection circuitry using Formula 3.1. Please note that it is the worst case scenario, when both diodes exhibit maximum leakage current.

$$\begin{aligned} V_{error} &= (R_{ser} \cdot (I_{bias} + I_{leak1} + I_{leak2})) \cdot A_u \\ &= (1k\Omega \cdot (250pA + 20nA + 20nA)) \cdot 1 \\ &= 40.25\mu V \end{aligned}$$

Of course, it is just a simple calculation that excludes such factors as temperature impact, tolerance of the resistor and so on. Having said that, the above-mentioned value is presented just to indicate the order of expected error.

Table 3.6: Parameters of OPA4180 taken from the manufacturer's datasheet [16]

Parameter	**Value**
Model	OPA4180
Manufacturer	Texas Instruments
Supply voltage	$\pm$2V to $\pm$ 18V
Bias current	250pA (typical)
Input offset voltage	75μV (maximum)
Drift voltage	0.1μV/ °C
Input voltage noise	$0.25\mu V_{pp}$
Slew rate	0.8V/μs

3.3.1.3 Signal conditioning

A first step in the signal capturing process was buffering. Now, the signal has to be conditioned in order to allow full range measurement without a risk of saturation of the analog-to-digital converter. As it can be imagined, the input range of popular mictrocontroller's analog inputs is usually up to 5V and more often up to 3.3V or even less once the external reference voltage source is used. This fact introduces a need of some attenuation and biasing. The second operation is required for the AC channel only. The circuit utilized for this purpose is presented in the Figure 3.7.

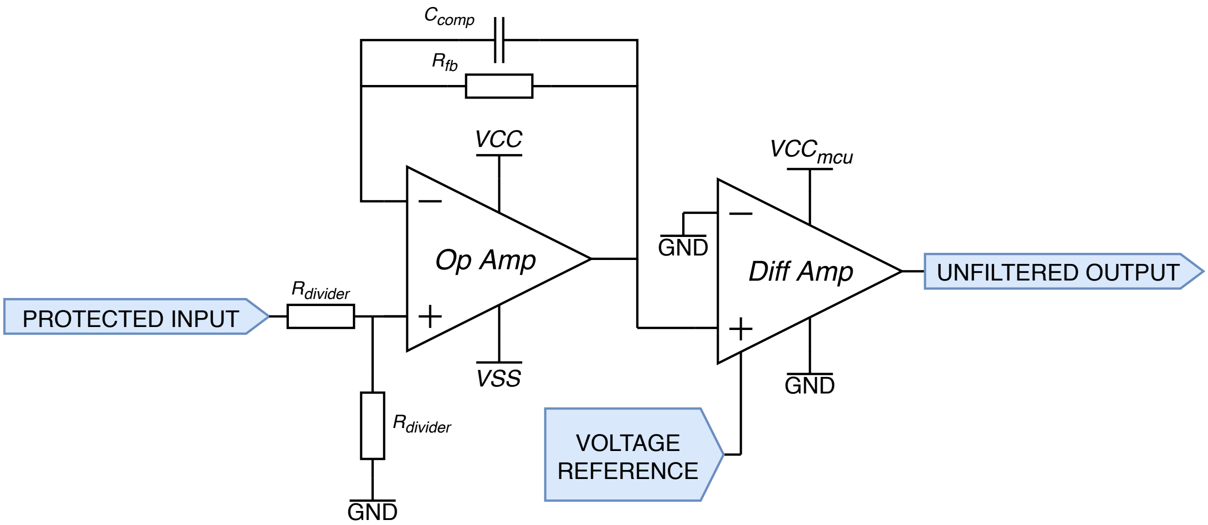

Figure 3.7: A circuit responsible for attenuation and level shifting

Attenuation is going to be performed by means of a voltage divider and the specialized differential amplifier. Unfortunately, there are a few problems associated with this solution. The first one is the excessive loading of the resistor network. Flowing current is going to generate losses in a form of heat. Any resistor has a parameter called temperature coefficient, which describes the resistance change in a function of temperature (usually in ppm/°C) [17]. High temperature coefficient components are undesired in precision electronics, thus designers should avoid them by all means. Temperature-related problems could be solved in a couple of different ways. In case of this design, the voltage divider would consist of low temperature coefficient resistors buffered with an operational amplifier. This solution would allow for a negligible current draw. The Op Amp used for this purpose is exactly the same as in case of the input buffer - see Table 3.6. The voltage divider need to provide a gain of 0.5. It would consist of two $10k\Omega$ resistors. Their temperature coefficient is as low as 25ppm. The resistance tolerance is 0.1% [18].

Additional attenuation is introduced by the differential amplifier - *INA159* by *Texas Instruments* - see Table 3.7 for its most important parameters. The resistor divider combined with the mentioned amplifier produce a fixed gain of 0.1, therefore it would be possible to capture input signals of $\pm$15V providing that the ADC is able to accept input voltages up to 3V (with proper biasing).

Table 3.7: Parameters of INA159 taken from the manufacturer's datasheet [19]

Parameter	**Value**
Model	INA159
Manufacturer	Texas Instruments
Supply voltage	1.8V to 5.5V
Gain	0.2
Gain accuracy	$\pm$0.024%
Input offset voltage	10μV (maximum)
Drift voltage	1.5μV/ °C
Bandwidth	15MHz
Slew rate	15V/μs

At this point, it is time to introduce the signal biasing. This process is absolutely necessary, since the microcontroller's analog-to-digital converter is unable to capture negative voltage. When adjusting the bias voltage, one should take into account both the input voltage range of the ADC as well as the reference voltage source, as its value determines the maximum signal level distinguishable by the microprocessor. By combining these informations, it is possible to notice that the bias voltage should be equal to the half of the reference voltage value. Happily, INA159 allows to maintain such conditions just by connecting the reference voltage source to one of its dedicated reference-related inputs [19].

3.3.2 DC channels section

The data acquisition board is equipped with three separate DC channels allowing to perform simultaneous measurements. These would be used to monitor sensors' response or inputs and outputs of particular DC converters associated with the piezoelectric generators. Owing to the fact that all of these channels can accept voltages exceeding the supply voltage of microcontrollers, some signal conditioning circuitry should be involved here as well.

3.3.2.1 Input protection

The input protection circuitry is exactly the same as described in the AC channel section.

3.3.2.2 Bufering

The buffering circuitry is exactly the same as described in the AC channel section.

3.3.2.3 Signal Conditioning

The input signal range of the DC inputs is 0-12V. Similarly as in case of the AC channel, the incoming signal ought to be conditioned to match the requirements of the ADC's input. In order to do so, the signal may need some attenuation, depending on its level.

The attenuation process is based on the resistor divider, exactly as before. The only difference is that the mentioned resistor network can be switched on and off depending on the input signal level. This way, the accuracy for low level signals is improved - see Figure 3.8. The resistor network can provide gain of 1 or 0.2, depending on the state of a MOSFET transistor. When considering the performance of resistors in the network, one should note that it is exactly the same as for the AC channel, for more details please refer to the datasheet of the manufacturer [18]. The buffer circuit is also exactly the same as in the previous case. For more information refarding the operational amplifier utilized in this circuit please refer to the OPA4180's datasheet [16].

Some care should be taken when selecting the MOSFET switch. It should be logic voltage level comparible and should provide low on-resistance. Both of these conditions are fulfilled by the NTJD5121NT1G [20]. By keeping the resistance of the divider in order of a few tens of $k\Omega$s and the R_{DSon} of 1-2Ω, it is possible to neglect the impact of the transistor.

Protection diodes are placed on the output of the circuit, as it is connected to low voltage section of the data acquisition board, this way unintended damage of some of the circuitry can be avoided.

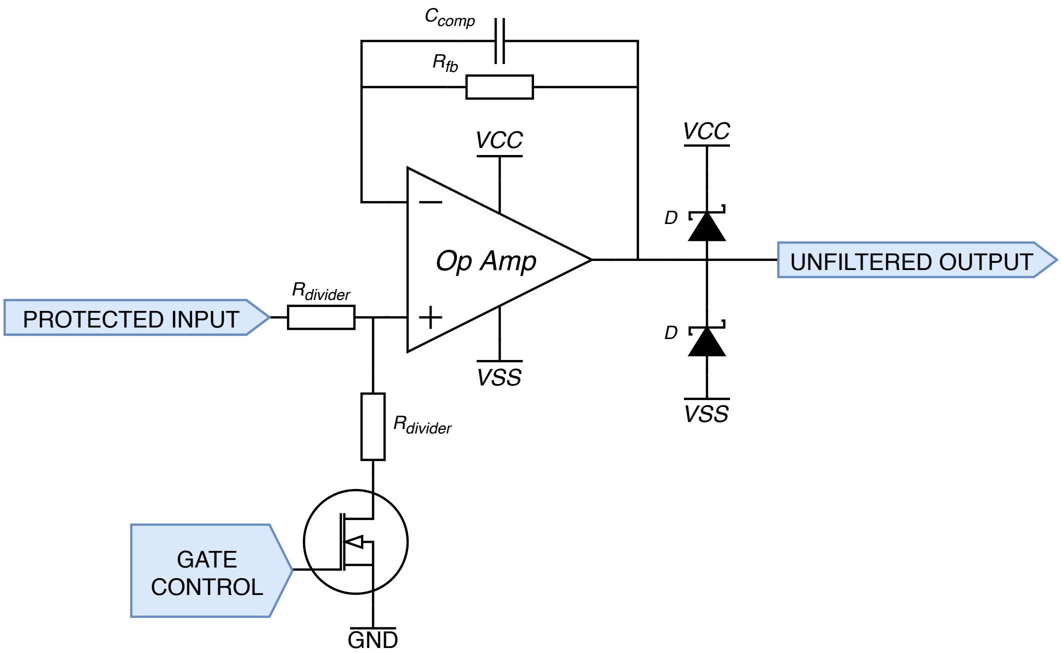

Figure 3.8: A circuit responsible for attenuation

3.3.3 *Anti-aliasing filter*

Anti-aliasing filters (AAFs) are utilized to restrict the bandwidth of the input signal. By placing the filter before the analog-to-digital converter, it is possible to remove high frequency noise and unwanted signals [21].

There are a few things that need to be taken info account when designing the AAF. The most important one is the bandwidth of the signal that should pass the filter undistorted. This information was already stated in the Table 3.2, so the maximum signal frequency is 500Hz. The second aspect of the filter design relates to its topology and order. Obviously, the higher order of the filter, the more complicated it is, therefore the design process should be a trade-off between the performance of the circuit and the complexity. By taking these aspects into account, it was decided to use the 2nd order Sallen-Key low-pass filter, as it combines decent performance with structure simplicity. Its topology is presented in the Figure 3.9.

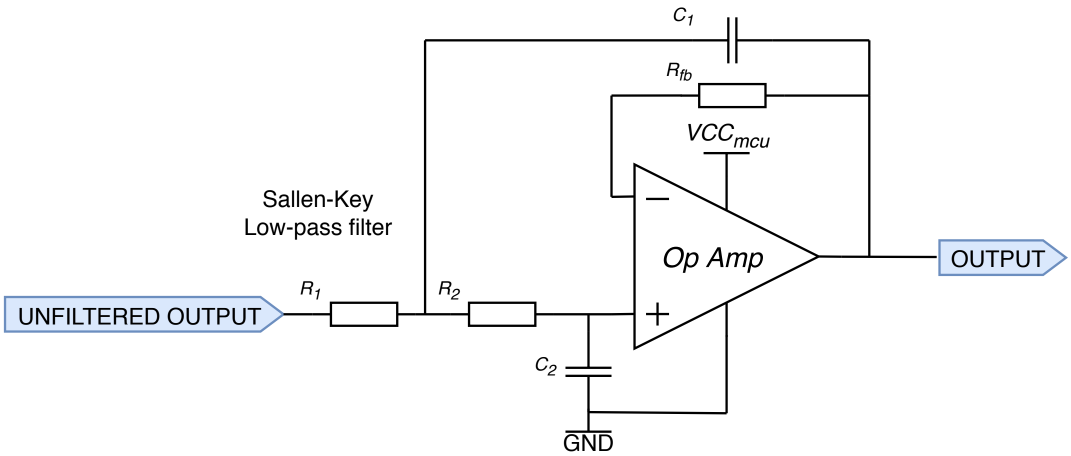

Figure 3.9: Anti-aliasing filter topology

Some literature [21] mention that the cut-off frequency f_c of the filter should be at least ten times higher than the signal frequency. Please note that square signals of 500Hz would require wider bandwidth than sine signals in order not to disturb sharp edges of the signal. Owing to this fact the cut-off frequency of the filter is going to be set at around 30kHz.

By selecting the same values for both R_1 and R_2 as well as C_1 and C_2, the formula for the cuf-off frequency f_c looks as follows:

$$f_c = \frac{1}{2 \cdot \pi \cdot R \cdot C} \tag{3.3}$$

where:

R – Resistance of R_1 and R_2,
C – Capacitance of C_1 and C_2.

Another important parameter associated with the filter is its quality factor Q. The quality factor informs about the stability of the filter as well as its response around the cut-off frequency.

$$Q = \frac{1}{3 - A} \tag{3.4}$$

where:

A – Voltage gain (for unity gain buffer A = 1)

By solving the above-mentioned equations, the following values are obtained:

$$f_c = \frac{1}{2 \cdot \pi \cdot R \cdot C} = \frac{1}{2 \cdot \pi \cdot 2.2k\Omega \cdot 2.2nF} = 32.833kHz$$

$$Q = \frac{1}{3-A} = \frac{1}{3-2} = 0.5$$

The cut-off frequency is found at around 33kHz, so the component selection was performed in the right way. The quality factor for the unity buffer in the second order filter configuration is always 0.5. It means that the filter is slightly underdamped, what could generate delicate overshoots and undershoots with rapid changing signals, but these would be negligible. The frequency response of the designed filter is presented in the Figure 3.10.

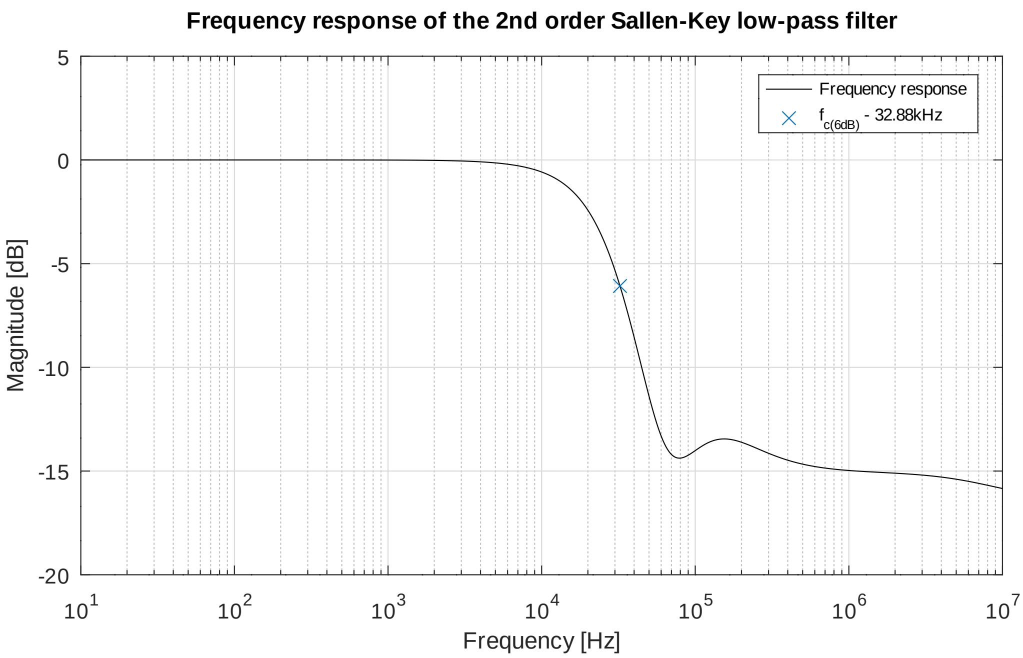

Figure 3.10: The frequency response of anti-aliasing filter based on 2nd order Sallen-Key configuration

3.3.4 Voltage reference

The reference voltage source is an important building block in precision analog electronics. Due to the fact that the designed board utilizes the analog-to-digital converter with resolution of at least 14-bits, it is important to follow particular design rules in order not to spoil its performance.

There are many different flavours of voltage reference sources, but the basic division includes zener and band-gap reference types [14]. Zener-based voltage incorporates a low-tempco zener diode and additional circuitry such as a matching silicon diode cancelling the influence of the temperature coefficient. Quite often, such references include internal heaters in order to maintain relatively stable temperature of the diode, therefore reducing the temperature impact. It is worth to highlight that such references may get quite expensive and very often offer only high reference voltage values, thus some additional circuitry may be required for interfacing the a microcontroller [14].

The second type of voltage reference sources is called the band-gap reference voltage. This type is based on matched transistors, and with some additional circuitry, it is able to provide lower (and precisely trimmed) reference voltages with comparable temperature coefficients. Moreover, such references may include internal buffer, thus no additional circuitry is often required [14].

The most important parameters of the voltage reference source are the mentioned temperature coefficient and output voltage tolerances. Due to the fact that band-gap references are readily available and offer suitable reference voltage levels, this type of solution would be considered in this design.

Table 3.8: Parameter of REF5030 taken from the manufacturer's datasheet [22]

Parameter	**Value**
Model	REF5030
Manufacturer	Texas Instruments
Temperature drift (max)	8ppm/°C
Output voltage tolerance (max)	0.1%
Output current (max)	10mA
Type	Band-gap
Reference voltage value	3.0V

3.3.5 Microprocessor selection

The microcontroller is a brain of the data acquisition board. As it can be imagined, it is responsible for such tasks as analog-to-digital conversion, data processing and communication with a personal computer. In addition, it is going to provide a basic user interface by means of buttons and switches for configuration purposes and signalling LEDs. Apart from that, there should be some space for calibration process, as well as triggering signals, thus additional I/Os would be included on the board for user-friendliness.

The Table 3.2 listed some of design requirements applicable for the MCU, namely, the ADC resolution as well as minimum sampling rate. In addition to that, the microprocessor has to be equipped with sufficient amount of inputs and outputs as well as communication interfaces in order to provide reliable connectivity with the PC.

Table 3.9: Features of MSP432P401R taken from the manufacturer's datasheet [23]

Parameter	**Value**
Model	MSP432P401R
Manufacturer	Texas Instruments
Architecture	32-bit ARM
Clock frequency	48MHz
Flash memory	256KB
SRAM memory	64KB
ADC resolution	up to 16-bit
ADC sampling rate	up to 1Msps
ADC input channels	up to 24
UART channels	4
UART max. baud rate	460800bps
SPI channels	4
SPI max. baud rate	16Mbps

By following mentioned requirements, the device presented in the Table 3.9 has been selected for this design. It is worth to highlight its superior analog features, namely the analog-to-digital converter capable of producing 16-bit results when the appropriate layout and averaging of recorded samples are implemented (the device incorporates a native 14-bit SAR core) [24]. Apart from analog-related features, the selected MSP432 provides numerous digital interfaces, what comes in handy when a connection with a personal computer is required. In this design, the primary communication channel would be based on UART, but is also planned to include an SPI-to-USB bridge for experimental purposes.

3.3.5.1 Architecture

Once the right microcontroller has been selected, one has to think about its peripherals required to allow easy connectivity as well as user-friendly interface. A general architecture of the designed system is presented in the Figure 3.11. In the following sections, all major sections would be briefly introduced.

3.3.5.2 ADC

The analog-to-digital converter is the most important part of the entire system. According to the manufacturer's description [23], the selected device is able to achieve 16-bit precision with software over-sampling. The sampling rate is resolution dependent and for 14-bit mode, MSP432 is able to provide 1Msps. It is vital to point out that for better precision, the external voltage reference source is used.

3.3.5.3 External voltage reference

As mentioned in the previous paragraph, the MCU is equipped with the external reference voltage source in order to improve stability of the ADC. The selected device (REF5030) provides such features as the accuracy as low as 0.1% and temperature drift lower than 8ppm/°C [22]. The built-in reference has only 1% accuracy and temperature drift up to 60ppm/°C [23]. MSP432 devices provide dedicated voltage reference input terminals (+VREF and -VREF) to facilitate the described modification.

3.3.5.4 User interface

The purpose of the data acquisition board is to allow easy and precise measurement of high impedance signals with a focus on piezoelectric-based circuits. The standard way of communication between the board and user is maintained by means of a personal computer, but there is some space for improvement.

It is planned to incorporate some basic functionalities based on switches and buttons. A 4-channel DIP switch is designated for configuration purposes. There are also two momentary buttons allowing to control the measurement process. An RGB LED is used for status indication.

In addition, there is a dedicated trigger pin that could be used to synchronize the board with a signal or with an external measurement instrument.

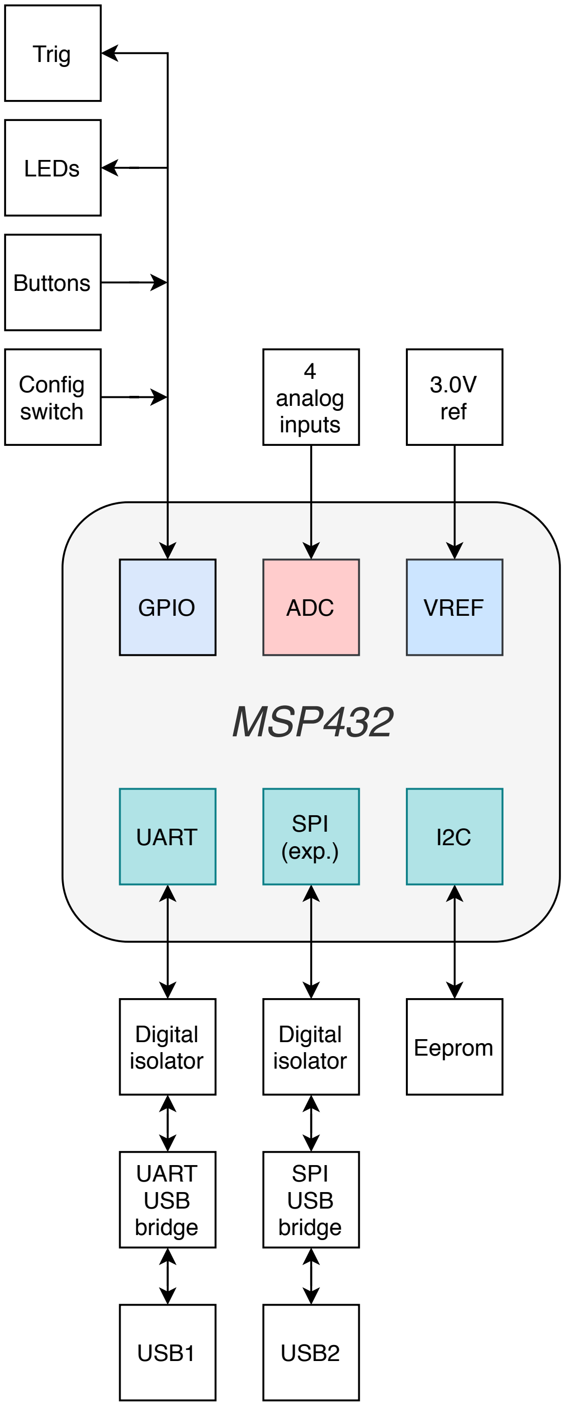

Figure 3.11: Architecture of the microcontroller and its peripherals

3.3.5.5 Connectivity

The designed device utilizes a few digital interfaces to communicate with peripherals and the personal computer. UART and SPI are used for data streaming and for parsing commands. I2C interface is used for communication with an EEPROM memory storing calibration constants and some basic info related to the device. At this point it is important to point out that SPI interface is for experimental purposes only, therefore UART is assumed to be the basic interface between the computer and the board.

Since the data acquisition module is glvanically isolated from the computer, all signals has to include additional isolating devices. In case of the UART, Rx and Tx signals are separated between primary and secondary side of the board by means of an Analog Devices ADuM1201 digital isolator. According to the manufacturer's datasheet [25], it supports data rates up to 25Mbps and 2500V RMS isolation for 1 minute per UL 1577. SPI interface is isolated using Maxim Integrated MAX14851 six-channel digital isolator. It is supporting data rates as high as 50Mbps and isolation of 600V RMS for 1 minute [26].

In order to make the device compatible with USB protocol, it is necessary to provide signal bridges for UART and SPI interfaces. This way, the user would be able to easily connect the data acquisition board directly to the personal computer. The USB-to-UART bridge parameters are stated in the Table 3.10. It supports baud rates up to 1Mbps, which makes it suitable fot this design. It is important to point out that CP2012 is fully compatible with most popular operating systems.

Table 3.10: Features of CP2102 taken from the manufacturer's datasheet [27]

Parameter	**Value**
Model	CP2102
Manufacturer	Silicon Labs
Max. baud rate	1Mbps
On-chip voltage regulator	3.3V
USB 2.0 compliant	Yes
Transmit buffer	640 bytes
Receive buffer	576 bytes
USB powered	Yes
Compatibility	Windows/Linux/Mac

The USB-to-SPI bridge is also manufactured by *Silicon Labs* - see Table 3.11. The most important features of this device are the maximum baud rate of 12MHz and 11 fully configurable GPIOs. Due to the fac2t that SPI is jut an experimental mean of communication is this project, there would be no more focus on SPI-related circuitry.

Table 3.11: Parameters of CP2130 taken from the manufacturer's datasheet [28]

Parameter	**Value**
Model	CP2130
Manufacturer	Silicon Labs
Max. SPI clock	12MHz
On-chip voltage regulator	3.45V
USB 2.0 compliant	Yes
Operation modes	3 or 4-wire
Configurable GPIOs	11
USB powered	Yes
Compatibility	Windows

4 ENERGY HARVESTER

The second part of this Master's project is to investigate the concept of vibrational energy harvesting. In the following chapter, the entire design process of a few different energy

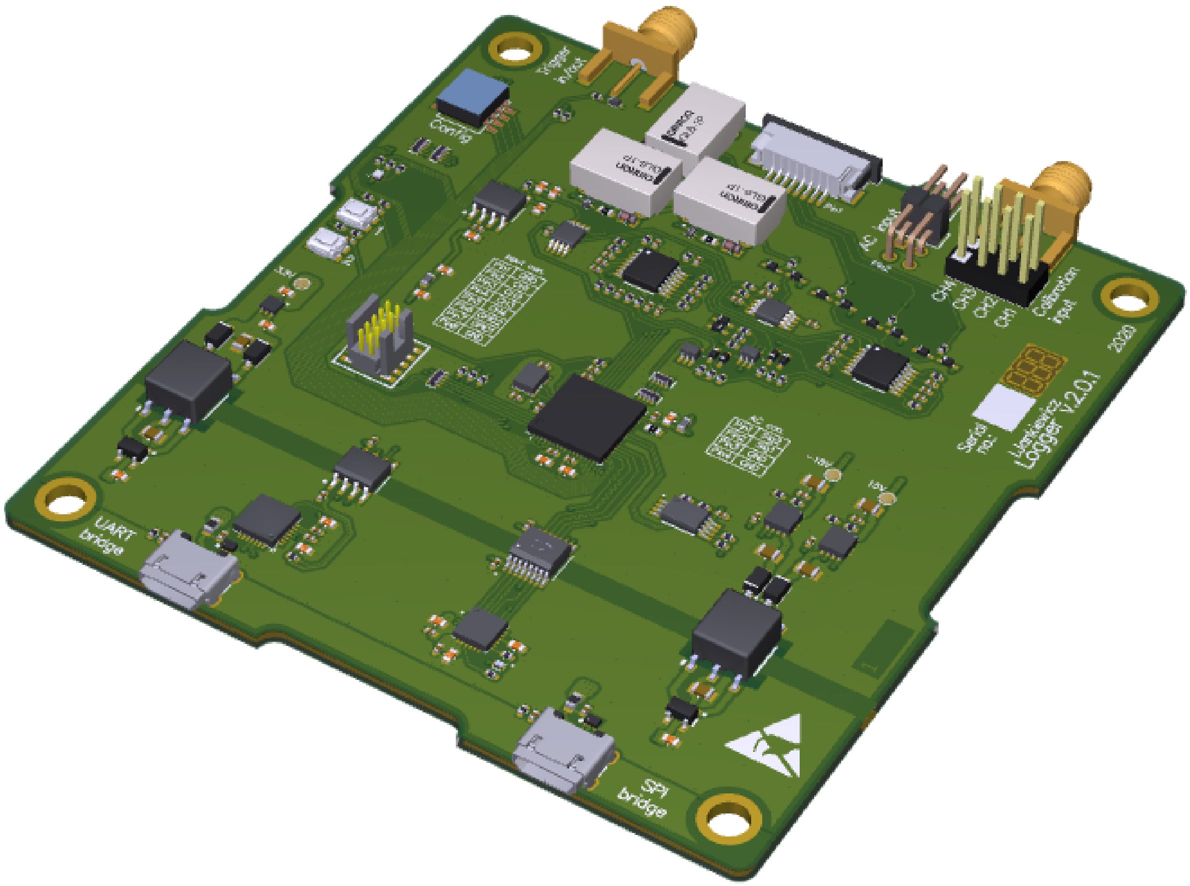

Figure 3.12: Data acquisition board 3D model

harvesters would be provided. In addition to that, there would be a number of different load circuits.

4.1 •

4.2 Energy harvesting integrated circuits

4.2.1 LTC3588-1

The *LTC3588-1* by *Linear Technology* is one of the most popular off-the-shelf solutions used in piezoelectic energy harvesting applications. Owing to the fact that target applications of such energy scavenging systems are focused on IoT devices, the described integrated circuit has one huge advantage in comparison to other devices, namely the solution size.

It's datasheet [29] states that to make the device work properly, only four capacitors and one inductor are required. Additional two resistors may be useful in order to set desired output voltage, but they are just an option. The simplified diagram of the described solution is presented in the Figure 4.1. It is worth to note that the solution size is greatly reduced by an integrated low-loss full-wave bridge rectifier that also makes a perfect fit for AC input signals.

Most important parameters of *LTC3588-1* are mentioned in the Table 4.1. Apart from the mentioned integrated rectifier, there are a few more features making this integrated circuit suitable for the job. The input voltage range easily covers values expected at the output of simple piezoelectric generators. Moreover, it included an overvoltage clamp protecting the device [29].

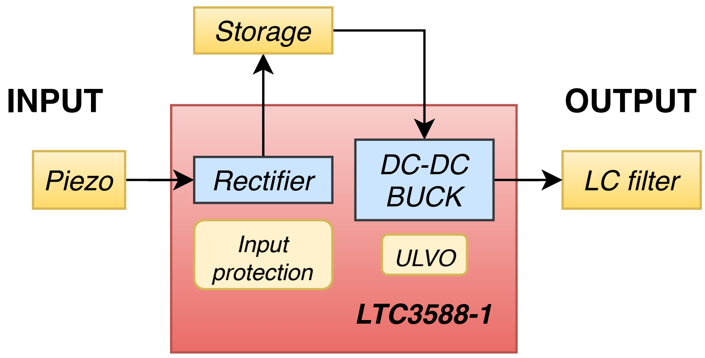

Figure 4.1: The diagram of *LTC3588-1* based energy harvesting system

Very low quiescent current of the device makes it possible to use just a supercapacitor as an energy storage element.

Table 4.1: Most important features taken from the manufacturer's datasheet [29]

Parameter	**Value**
Model	LTC3588-1
Manufacturer	Linear Technology
Input operating range	2.7V to 20V
Quiescent current	950nA
Output current	up to 100mA
Selectable output voltages	1.8V, 2.5V, 3.3V, 3.6V
Input protection	Shunt type (up to 25mA Pull-down)
Undervoltage lockout	Yes
Integrated rectifier	Yes

4.2.1.1 Circuit design

When designing low power circuits, great care has to be taken about proper storage components, as these are the key to maintain an uninterrupted output of these circuits. The input capacitor is responsible for providing sufficient amount of energy for the DC-DC converter. On the other hand, the output capacitor determines the time interval for which the converter sleeps [29]. The exact size of mentioned components is mostly dependent on a particular application. Therefore, manufacturer's recommendation would be a reference in case of this design. Please note that selected components are supposed to meet voltage rating requirements, namely at least 20V for the input capacitor and 6.3V for the output capacitor. Based on these details, the following components have been picked:

Table 4.2: Capacitors selected for the *LC3588-1* circuit [30], [31]

Type	**Manufacturer**	**Model**	**Capacitance**	**Rated voltage**	**Count**
Input	Würth Elektronik	865060442002	22μF	25V	1
Output	AVX	12066C226MAT2A	22μF	6.3V	3

When it comes to the inductance, the manufacturer advises to pick any value between 10μH and 22μH. Larger inductors can be beneficial in high voltage applications [29]. The selected component should have a DC current rating of 350mA or more. Please note that DC resistance of the inductor has an impact on the overall efficiency of the converter.

Table 4.3: Inductor selected for the *LC3588-1* circuit [32]

Manufacturer	Model	Inductance	Rated current	DC resistance
Würth Elektronik	74438335220	22μH	0.6A	1.04Ω

Figure 4.2 presents the layout of the described circuit. Apart from previously mentioned components, there is also a DIP switch allowing to configure the output voltage of the converter. This way, the DC-DC converter could be easily adjusted by the user according to the table printed on the silkscreen.

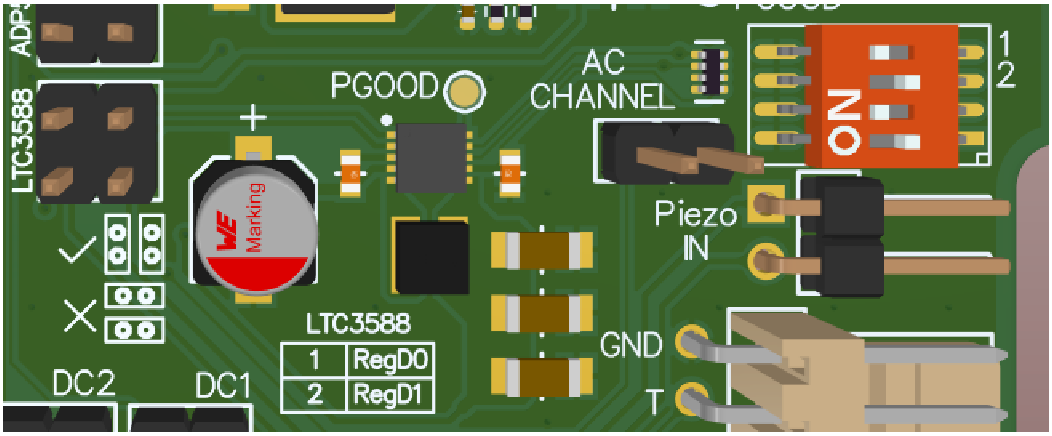

Figure 4.2: The layout of *LTC3588-1* based circuit

4.2.2 *LTC3331*

The most complicated of integrated circuits selected for this design is *LTC3331* by *Linear Technology*. It takes advantage of a few features very similar features to those described in the section focused on *LTC3588-1*, but its performance is extended. This notion would be described further in the following section.

The *LTC3331* is a smart energy harvester that includes two DC-DC converters, a battery charger, a supercapacitor balancer and an input protection circuitry [33]. This device is dedicated for multiple alternative energy sources including solar, thermal and piezoelectric sources. A huge advantage of this integrated circuit is an integrated full bridge rectifier, exactly as in case of the *LTC3588-1* provided by the same manufacturer. The another significant similarity is the input protection circuit clamping any input overvoltage events. According to the manufacturer's datasteet [33], targer application of circuits based on *LTC3331* are solar powered systems, security devices, wireless sensors and of course energy harvesters.

The Figure 4.3 presents the overall structure of the described integrated circuit. As it can be seen, the input stage consists of the integrated rectifier and the storage capacitor. The output stage is suportted by two DC-DC converters. The main one is the Buck converter, which is used to provide stable output based on harvested energy. This converter requires relatively stable input power source to operate properly. The second DC-DC converter takes advantage of the Buck-Boost topology. It is used to support the stability of the output voltage in cases when the harvester is not able to keep up with the power consumption of the load [33]. In addition to that, the *LTC3331* provides a battery charger capable of charging batteries with current up to 10mA.

The output could be further supported by the storage supercapacitor. One should remember that most of these devices exhibit very low voltage ratings, so it is often necessary to connect them in parallel. For this occasion, the harvester provides a supercapacitor balancer supporting balance currents as high as 10mA [33].

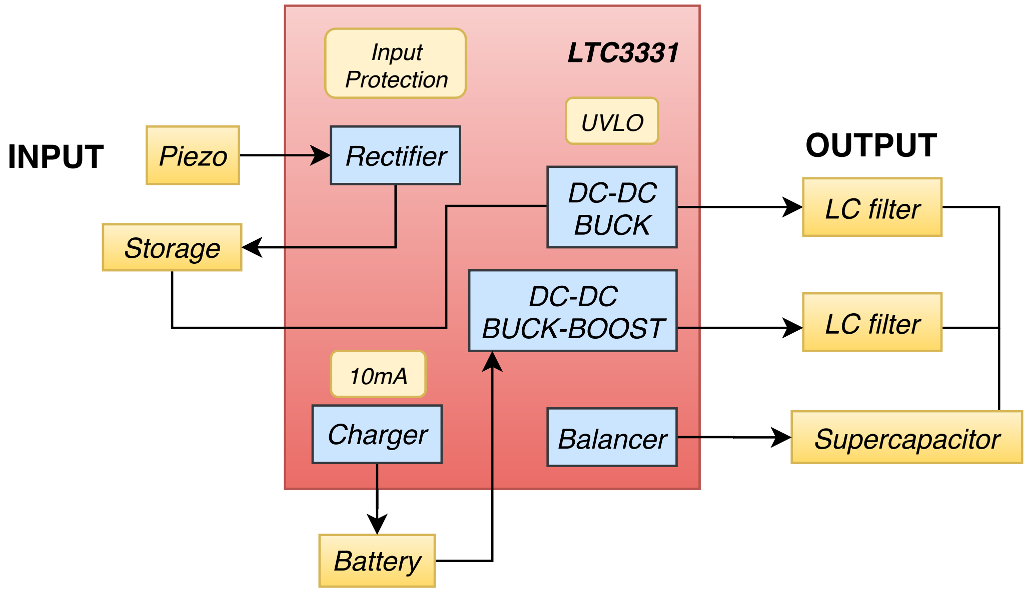

Figure 4.3: The diagram of *LTC3331* based energy harvesting system

The Table 4.4 lists the most important feature of the described integrated circuit. The input voltage range is broad enough to cover most of expected voltage values generated by piezoelectric harvesters. Moreover, the quiescent current of the device is very low, therefore the storage component is not excessively drained. The voltage drop of the integrated rectifier also helps to maintain high efficiency.

Table 4.4: Most important features taken from the manufacturer's datasheet [33]

Parameter	**Value**
Model	LTC3331
Manufacturer	Linear Technology
Input operating range	2.7V to 19V
Quiescent current	950nA
Output current	up to 50mA
Selectable output voltages	from 1.8V to 5.0V
Input protection	Shunt type (up to 25mA Pull-down)
Undervoltage lockout	Yes (adjustable)
Integrated rectifier	Yes
Rectifier total drop	800mV(at 10μA)
Battery charger max. current	10mA
Balancer max. current	10mA

4.2.2.1 Circuit design

During the design process of the *LTC3331* based circuit, the manufacturer's datasheet [33] was a reference.

Firstly, proper inductor has to be selected. The Buck converter is optimized for 22μH inductors. Nevertheless, it is possible to pick a higher value of inductance in order to increase the efficiency of the DC-DC Buck converter in high voltage applications [33]. One should note that the DC resistance of the inductor has an impact on the overall efficiency of the converter. When it comes to the Buck-Boost converter, the manufacturer claims that the recommended inductance value is also 22μH. Please note that it is allowed to pick the another inductor, but the peak current of the inductor need to be adjusted by setting some of the integrated circuit's pins high or low - see the datasheet [33]. For this occasion, a DIP switch has been installed. Eventually, the same inductor model has been selected for both converters. Its parameters are listed in the Table 4.5.

Table 4.5: Inductor selected for the *LTC3331*'s Buck and Buck-Boost converters [34]

Manufacturer	Model	Inductance	Rated current	DC resistance
Coilcraft	LPS4012-333	33μH	0.46A	0.825Ω

The decision of using the larger value of inductance than the one recommended by the manufacturer is mostly due to the fact that the input voltage level of the Buck converter is currently unknown. As it was mentioned before, the higher inductance values increase the efficiency of the converter at higher input voltages, so the trade-off has been made. As to the Buck-Boost converter, it is possible to adjust the peak inductor current value, so there is no problem using higher inductances.

When it comes to selection of suitable capacitors, the datasheet [33] also served as a reference. The input capacitor's recommended value depends on the input current generated by the piezoelectric element. By varying its value, it is possible to tune the harvester to maximize the amount of harvested energy. As a starting point, the input capacitor's value is set to 22μF, as this value has been proposed by the manufacturer in various reference designs.

When considering the output capacitor, the situation is almost the same, since the ripple current of the output capacitor depends on both the load and the amount of energy provided by the piezoelectric beam. One should remember to choose low inductance ceramic capacitors in SMD packages in order to minimize high frequency ripple introduced by the DC-DC converter [14]. At the prototyping stage, three 22μF ceramic capacitors has been connected in parallel, but this configuration could be a subject of change. Details in the Table 4.6.

The purpose of the battery capacitor is to minimize the voltage droop when using the Buck-Boost converter [33]. Having said that, it is important to place it relatively close to the integrated circuit in order to provide low impedance path for the converter's input [14]. The manufacturer's advice is to use 4.7μF or greater in order to maintain the performance [34]. In this design, two general purpose 10μF tantalum capacitors in parallel has been chosen for this job, as they provide good compromise between capacitance and size. More details are included in the Table 4.6.

Table 4.6: Capacitors selected for the *LTC3331* circuit [31], [30], [35]

Type	Manufacturer	Model	Capacitance	Rated volt.	Count
Input	Würth Elektronik	865060442002	22μF	25V	1
Output	AVX	12066C226MAT2A	22μF	6.3V	3
Battery	AVX	TAJA106M010RNJ	10μF	10V	2

The layout of the designed circuit is presented in the Figure 4.4. Similarly to the previous harvester, it is possible to change most of the settings of the integrated circuit by means of included DIP switches. This way, the evaluation of the *LTC3331*

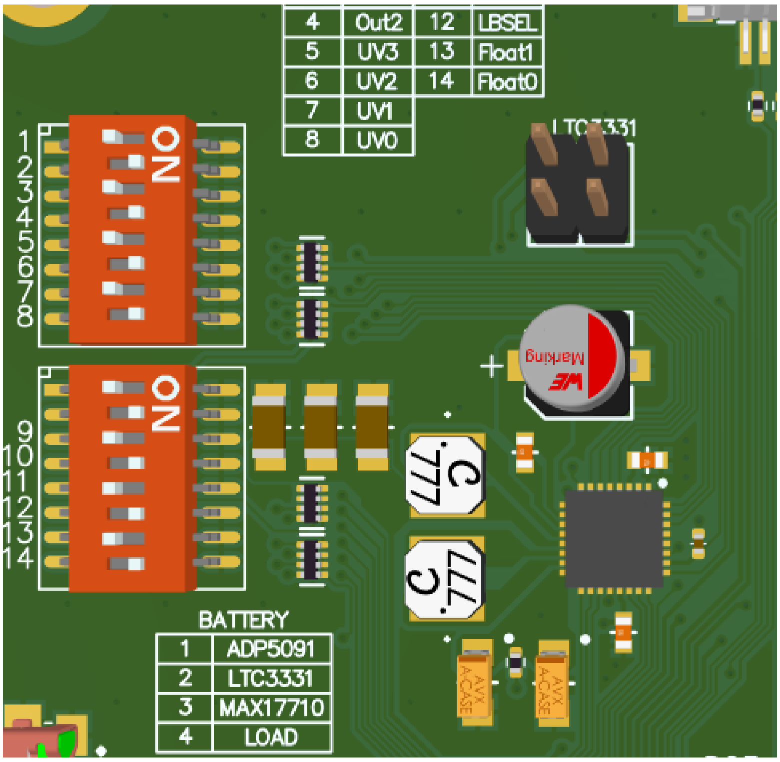

Figure 4.4: The layout of *LTC3331* based circuit

4.2.3 ADP5091

Another alternative for an integrated energy harvester is *ADP5091* by *Analog Devices*. This device is not dedicated exclusively for vibration energy harvesting applications. In case of piezo-based applications, it is necessary to provide an external voltage rectifier, as the described integrated circuit accepts only DC voltage at the input. One should note that *ADP5091* incorporates a DC-DC boost converter and LDO, which is optimized for high efficiency at low output currents [36].

Figure 4.5 depicts the overall structure of the harvester. As mentioned before, the device is compatible with DC sources only. Having said that, it is necessary to perform input voltage conditioning by means of an external voltage rectifier. To further smooth the voltage, a storage capacitor is to be installed. Once the input voltage is rectified, the *ADP5091* is able to perform a DC conversion in order to provide regulated output voltage. The described integrated circuit is combining two different voltage regulators, namely the LDO and the DC-DC Boost converter. In case of this design, only Boost converter would be used. Nevertheless, it is possible to select the hybrid operation mode, where both of regulators are used alternatively depending on the actual performance of the input power source[36].

Due to the fact that the *ADP5091* takes advantage of the DC-DC boost converter, this configuration is dedicated for low output voltage piezoelectric generators. Table 4.7 lists the most important parameters of the device.

One should note relatively low input voltage operating range. In order to face this problem, it may be required to use a relatively high input capacitance that would impose more load on the piezoelectric generator, therefore reducing its output voltage [2]. The *ADP5091* has remarkably low quiescent current, what is one of the most important aspects in energy harvesting

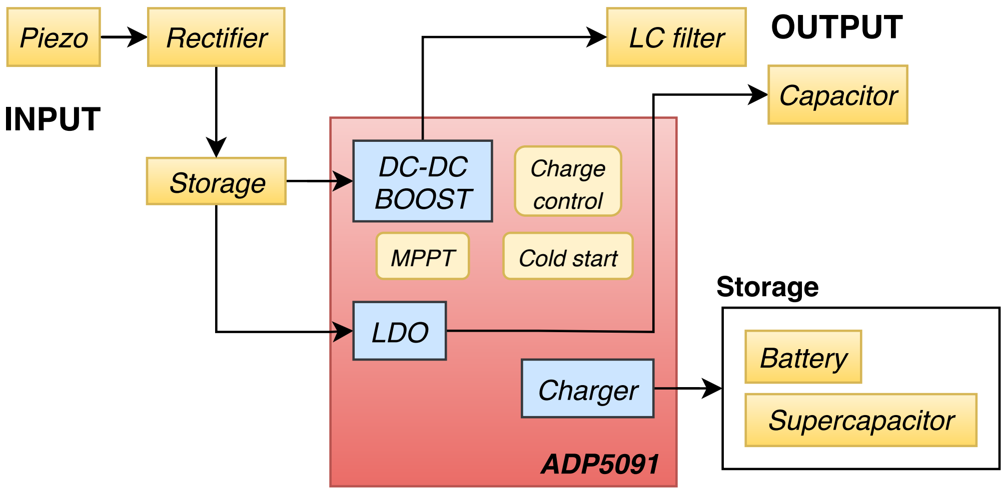

Figure 4.5: The diagram of *ADP5091* based energy harvesting system

Table 4.7: Most important features taken from the manufacturer's datasheet [36]

Parameter	**Value**
Model	ADP5091
Manufacturer	Analog Devices
Input operating range	0.08V to 3.3V
Quiescent current	510nA (typical)
Output current	up to 150mA
Selectable output voltages	from 1.5V to 3.6V
Integrated rectifier	No
Fast Cold Start threshold voltage	380mV
Optional back-up	Yes (primary battery)
MPPT	Yes

applications. In addition to that, the manufacturer claims it provides an MPPT feature. The input voltage threshold is as low as 380mV, what makes it possible to maximize the amount of harvested energy.

4.2.3.1 Circuit design

The selected inductor should have saturation current at least 30% higher than the peak inductor current (which might be as high as 300mA) and relatively low DC resistance in order to maintain high efficiency [36]. The converter is optimized for 22μH inductors. By combining all mentioned parameters, the inductor listed in the Table 4.8 has been selected.

Table 4.8: Inductor selected for the *ADP5091* circuit [37]

Manufacturer	**Model**	**Inductance**	**Rated current**	**DC resistance**
Würth Elektronik	744042220	22μH	0.88A	0.3Ω

Input capacitor is utilized to store energy captured from the piezoelectric beam. Its value recommended by the manufacturer is at least 10μF, but larger values may be beneficial in case when an additional primary battery is used [36]. In case of this design, the minimum recommended value would be a way to go.

The output capacitor is used to smooth the output voltage of the switching regulator. Even though, the minimum recommended value is 4.7μF, it would be extended to 22μ to further smooth the output voltage. There are a few more capacitor required by the integrated circuit to operate properly, but all of them would be picked according to the manufacturer's recommendations. Please see Table 4.9 for details regarding input and output capacitors.

Table 4.9: Capacitors selected for the *ADP5091* circuit [30], [35]

Type	Manufacturer	Model	Capacitance	Rated voltage	Count
Input	AVX	TAJA106M010RNJ	10μF	10V	1
Output	AVX	12066C226MAT2A	22μF	6.3V	1

The last important aspect to mention is related to the full bridge rectifier's diodes. Owing to the fact that the forward voltage drop of these components has a huge impact on the overall efficiency of the power management circuit, one should select diodes suitable for this application. The designer's choice is placed in the Table 4.10. Please note that the forward voltage drop of these diodes conducting low current might be way lower than 200mV [38].

Table 4.10: Rectifier diodes selected for the *ADP5091* circuit [38]

Manufacturer	Model	Forward voltage ($I_f = 500mA$)	Forward Current
Nexperia	PMEG4005EJ	0.42V	0.5A

The layout of the *ADP5091*-based circuit in presented in the figure 4.6. One should note a DIP switch that makes it easy to change some of the inegrated circuit's settings. This feature is particularly useful during the circuit evaluation process.

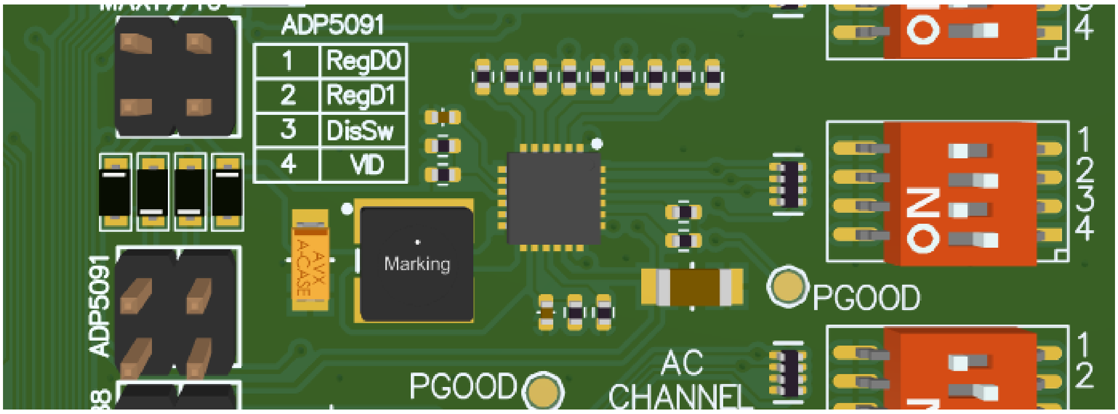

Figure 4.6: The layout of *ADP5091* based circuit

4.2.4 *MAX17710*

The last of selected devices is *MAX17710* by *Maxim Integrated*. It is a complete system for charging and protecting small storage devices [39]. The manufacturer claims that the device can handle generators with output power levels as low as 1μW. The output of the regulator is based on the very low quiescent current LDO, which also incorporates overdischarge protection of the battery.

The figure 4.7 presents the most important features of the described device. In case of this design, only the low-dropout regulator would utilized according to the manufacturer's recommendations [39], thus the DC-DC Boost converter is not mentioned in the diagram. The input

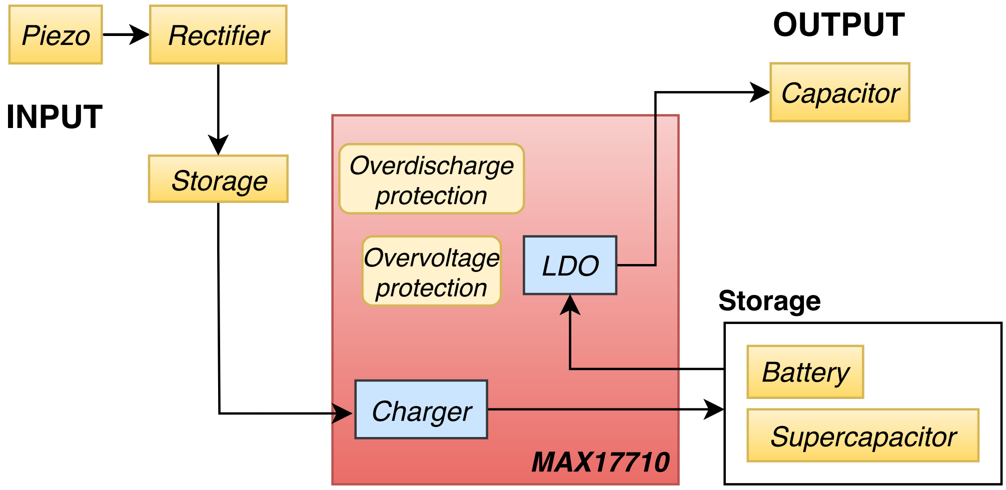

Figure 4.7: The diagram of *MAX17710* based energy harvesting system

part looks similar to the one described in the section regarding *ADP5091*. Due to the fact that *MAX17710* requires DC voltage at the input, the full bridge rectifier along with the storage capacitor are installed. The input power is used to charge the storage component, which could be both a rechargeable battery or a supercapacitor. Once there is a sufficient amount of charge stored, the LDO is able to source the output. The output voltage level can be adjusted according to the user's needs. In case the input charging voltage is higher than the allowed storage element voltage, the entire power is sourced to the LDO. Moreover,the device features the input overvoltage protection formed by a shunt diode. The storage component is also protected against over-discharge conditions [39]. Some of the most important features of the device are once again summarized in the Table 4.11.

Table 4.11: Most important features taken from the manufacturer's datasheet [39]

Parameter	**Value**
Model	MAX17710
Manufacturer	Maxim Integrated
Maximum Input Voltage	5.3V
Quiescent current	626nA (during charging)
Output current	up to 75mA
Selectable output voltages	from 1.8V to 3.3V
Integrated rectifier	No
Over-voltage protection clamping current	up to 50mA
Maximum Charging Current	100mA

Similarly to other described integrated circuits, *MAX17710* has significantly low quiescent current, what allows for energy harvesting using power sources with output capabilities as low as 1μW. Another interesting feature is the shunt input protection capable of clamping up to 50mA.

4.2.4.1 Circuit design

The following paragraph is describing the circuit design process. As usual, the manufacturer's datasheet [39] would be a main reference. Due to the fact the DC-DC Boost converter functionality is not used in this design, the component selection would be greatly simplified. When it comes to picking capacitors for the input and output of the regulator, one should take on the charge input of the device that is tied directly to the power source. The manufacturer's advice is to use a 100nF capacitor to maintain the highest efficiency, but for better stability from a high voltage source, a 220nF one should be used instead [39]. The output capacitance should be alt leat 1μF. The final choice is a 4.7μF to further smooth the output voltage. The Table 4.12 present more details.

Table 4.12: Capacitors selected for the *MAX17710* circuit [40], [41]

Type	Manufacturer	Model	Capacitance	Rated voltage	Count
Input	Würth Elektronik	885012105002	220nF	6.3V	1
Output	Würth Elektronik	885012106012	4.7μF	10V	1

The full bridge rectifier placed at the input of *MAX17710* consists of exactly the same diodes as those that have been used in the *ADP5091*-based circuit. For more details, please refer to the Table 4.10.

The layout of the designed circuit is presented in the Figure 4.8. One should notice its simplicity, what by all means is a huge asset in case of IoT designs or other small-form factor applications. The same as in case of other described designs, a DIP switch is utilized to easily change the settings of the integrated circuit. This solution would surely help to evaluate the circuit properly.

Figure 4.8: The layout of *MAX17710* based circuit

4.3 *Selection of load circuits*

An important part of the evaluation process is to provide proper load conditions for the harvester. By doing that, it is possible to find the maximum power point where the power source impedance matches the load, according to the maximum power transfer theorem [42].

The designed harvester board allows to use a few energy harvesters that could be connected to different types of loads.

4.3.1 *Utilizing storage components as the non-linear load*

Devices powered by energy harvesters usually require some kind of a storage element in order to maintain an uninterrupted power supply for its circuits in any conditions. Unfortunately, these components are not able to provide constant impedance. Moreover, it is often way too low to match the impedance of the power source.

One way of dealing with this problem is to take advantage of application-specific integrated circuits described in the previous part of this thesis. Many of them are able to alter the impedance of the load seen from the power source's contacts. This way, it would be possible to charge a battery or a supercapacitor without overloading the piezoelectric beam too much.

Figure 4.9 presents the layout of the printed circuit board including mentioned storage components. There is one lithium-polymer battery and two different supercapacitors. When it comes to the battery, it is exactly the same as the one utilized in the accelerometer board - for more details see Table 4.13.

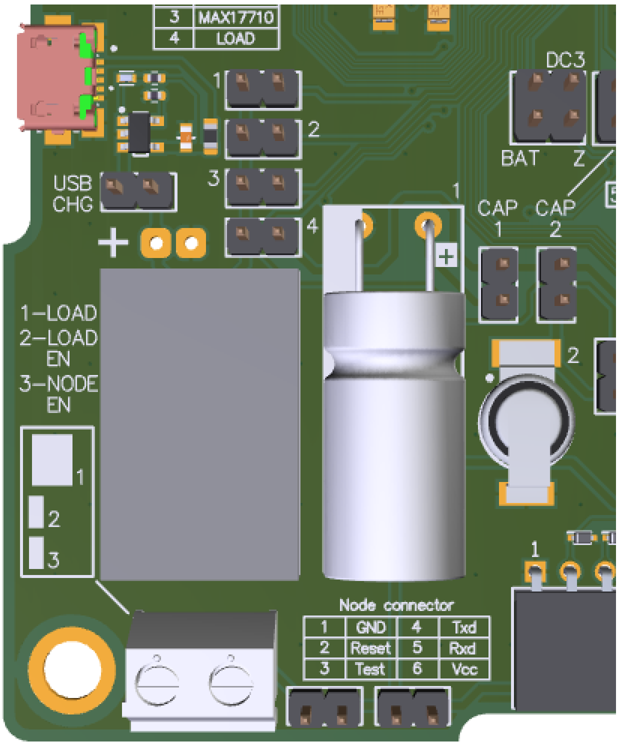

Figure 4.9: Li-ion battery and supercapacitors as a part of the load for energy harvesters

Table 4.13: Parameters of the lithum-polymer battery indealled on the PCB [43]

Parameter	Value
Manufacturer	Maxpower Idustrial
Model	Lipo511422
Capacity	110mAh
Nominal voltage	3.7V (1C)
Protection circuitry	yes

Some of the devices, such as *LTC331*, *ADP5091* and *MAX17710* provide dedicated battery chargers. The selected battery, due to its compact size and capacity that perfectly fits energy harvesting applications would be very helpful when evaluating the proposed design.

Another mean of storage component proposed in the project is the supercapacitor. For the sake of this project, there would be two different components installed. The major differences between them include rated capacitance, nominal voltage and internal impedance. Supercapacitors are becoming increasingly popular in low power designs owing to durability, low price and small dimensions. On the other hand, these devices can provide a few problems, such as relatively low rated voltage or a need of using special supercapacitor chargers in most of the cases.

The first of the selected capacitors is dedicated for energy harvesting applications. Its parameters are listed in the Table 4.14. It provides relatively large capacitance of 4.7F. Due to low internal resistance, it should not be charged directly by high output impedance sources, as it would cause severe impedance matching problems affecting the efficiency of energy transfer.

Table 4.14: Parameters of the first supercapacitor utilized as the load [44]

Parameter	**Value**
Manufacturer	Samxon
Model	DRL475S0TG20RRASP
Capacitance	4.7F
Nominal voltage	2.7V
Internal resistance (Ω) at 1kHz	0.14Ω

The second of selected components is designed for low power energy storage with the focus on memory power backup and similar. Please see Table 4.15 for more details. Even though the manufacturer does not mention energy harvesting as one of potential applications, the parameters of the component allow to assume that it would be a good fit. One should notice nominal voltage of the supercapacitor, that is a bit higher that 2.7V, making it more compatible with the harvesters utilized in this design. The internal resistance, though significantly higher than in the previous case, still is way lower then the output impedance of the power source, therefore its performance is expected to be similar.

Table 4.15: Parameters of the second supercapacitor utilized as the load [45]

Parameter	**Value**
Manufacturer	Elna
Model	DSK-3R3H224U-HL
Capacitance	0.22F
Nominal voltage	3.3V
Internal resistance (Ω) at 1kHz	200Ω

In addition to the above-mentioned features, the harvester board also allows to connect a custom load. In order to do so, the screw terminal has to be used - see the left bottom corner in the Figure 4.9. This way, it is easy to use a decade resistance box for proper impedance matching, thus maximizing the power transfer.

4.4 Microprocessor node as the active load

Most of the times, energy harvesting are intended to power low power electronics systems in order to make them energy self-sufficient. Having said that, one should consider this subsection as the reference point when analyzing the usefulness of piezoelectric energy harvesters as power sources for small microprocessor systems.

5 HARDWARE ASSEMBLY, TESTING AND CALIBRATION

In the following section, the assembly and testing procedure would be presented. All printed circuit boards were manufactured in China by a professional manufacturer. All electronic components were obtained from trusted vendors in order to make sure the performance

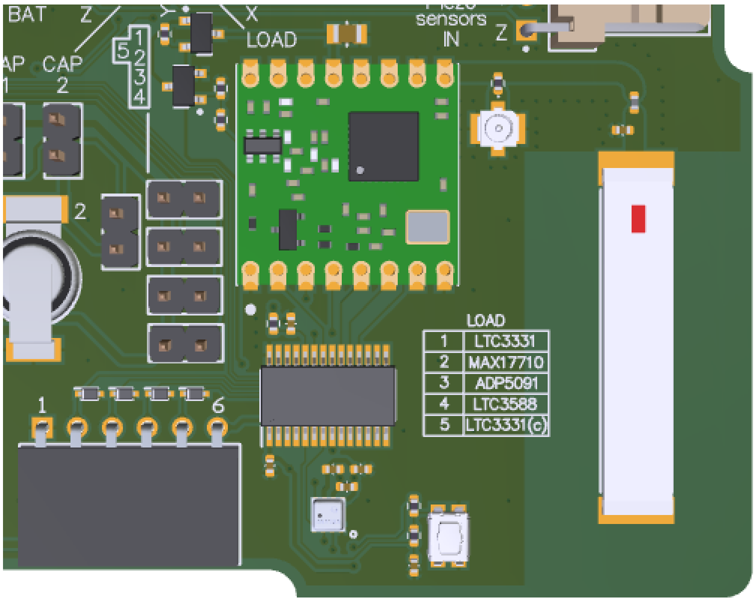

Figure 4.10: A microcontroller node as an active load for energy harvesters

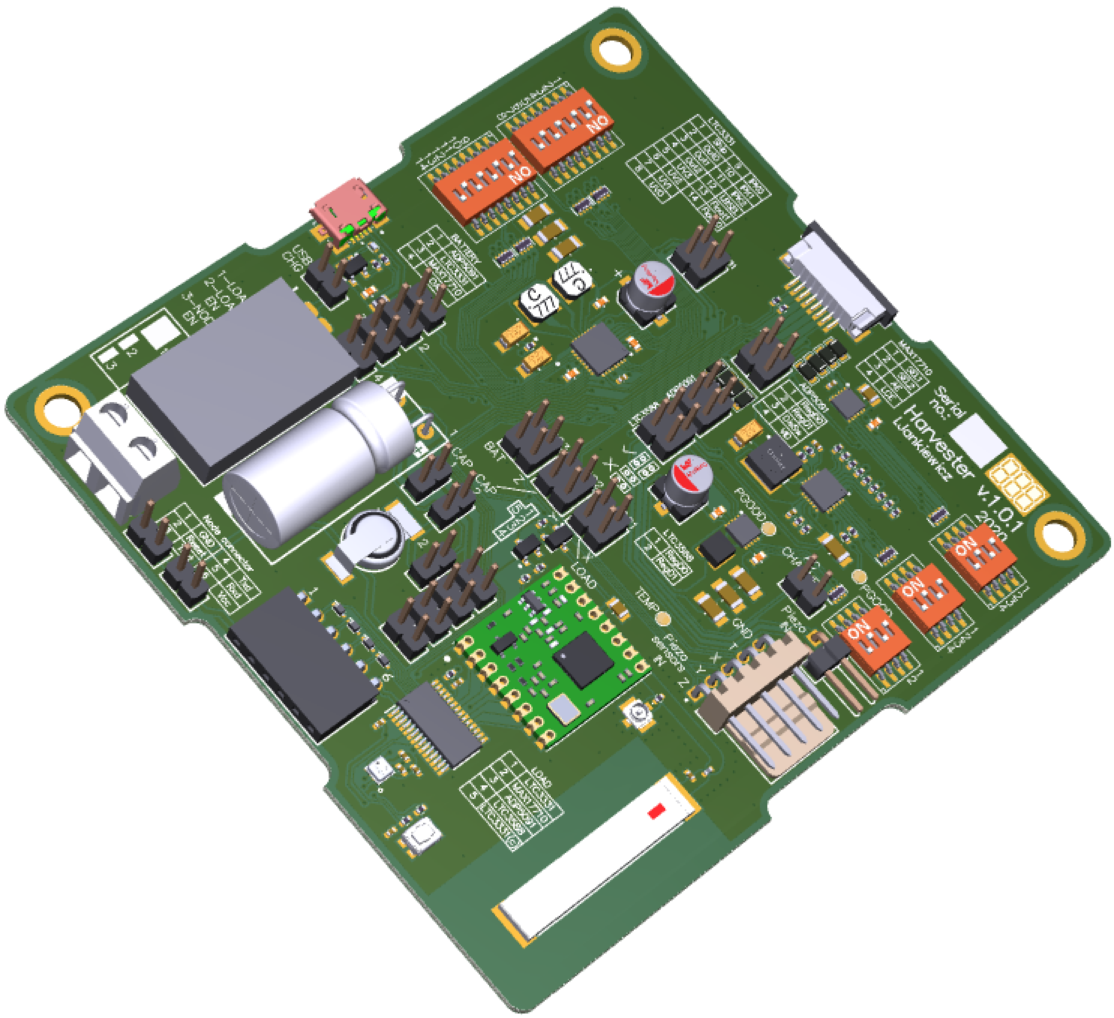

Figure 4.11: Harvester board 3D model

of all boards is optimal. Calibration process and testing was performed using laboratory equipment with the focus on a Keithley 2000 6.5 digit multimeter as a trusted reference.

5.1 Hardware assembly results

Figure 5.1 presents the assembled data acquisition board. The soldering process was performed using a vaporphase oven in order to get the best final results. The same applies to the harvester board presented on the Figure 5.2.

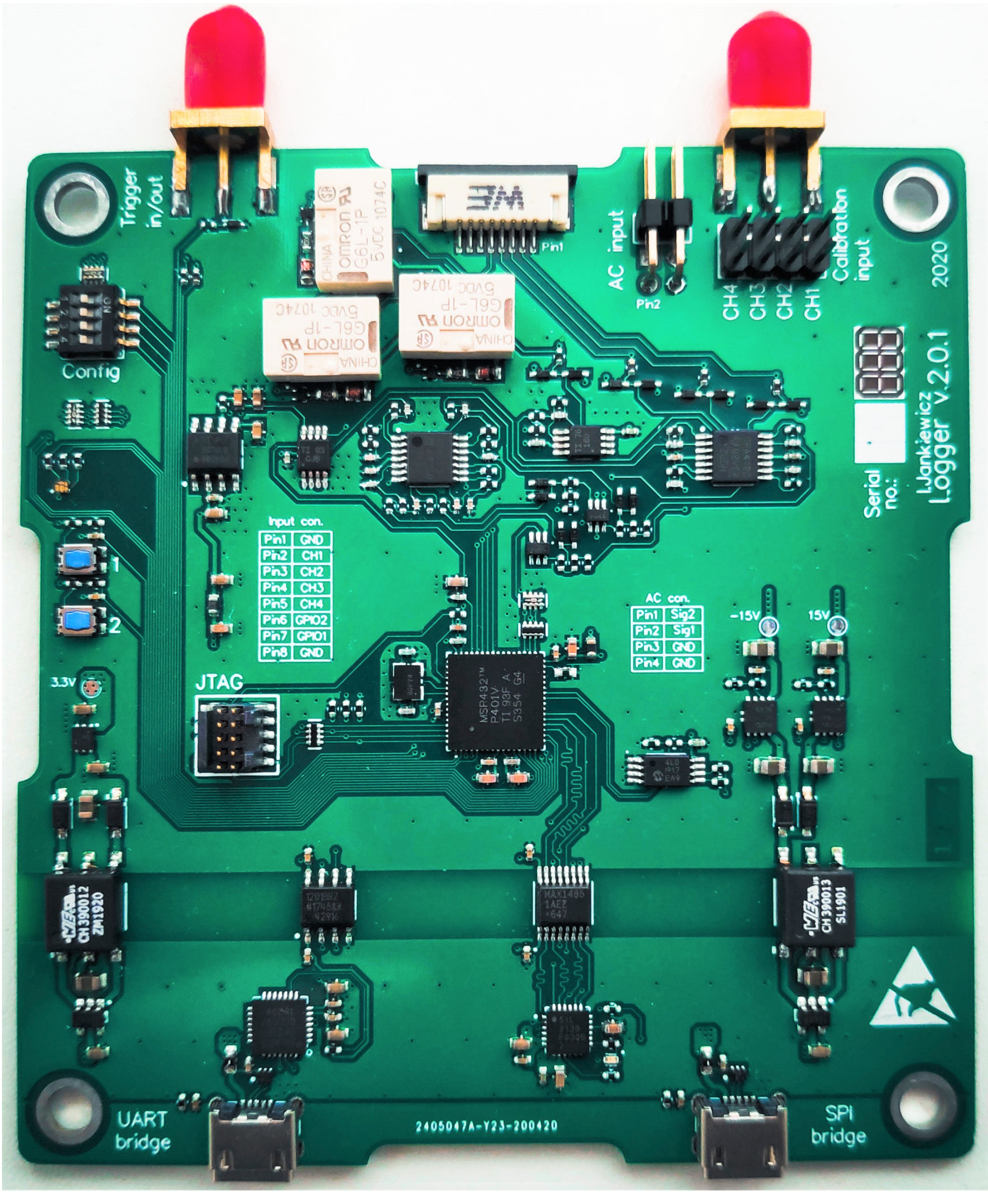

Figure 5.1: Assembled Data Acquisition board

Once the soldering in the oven was done, boards were examined using a microscope in order to track unwanted solder bridges or improper solder joints.

The next part of the process was to hand solder all through hole components. Once this step was done, both boards were attached to each other by means of M4 screws and metal distances. All electrical connections are established using the FPC tape connector as presented in the Figure 5.3.

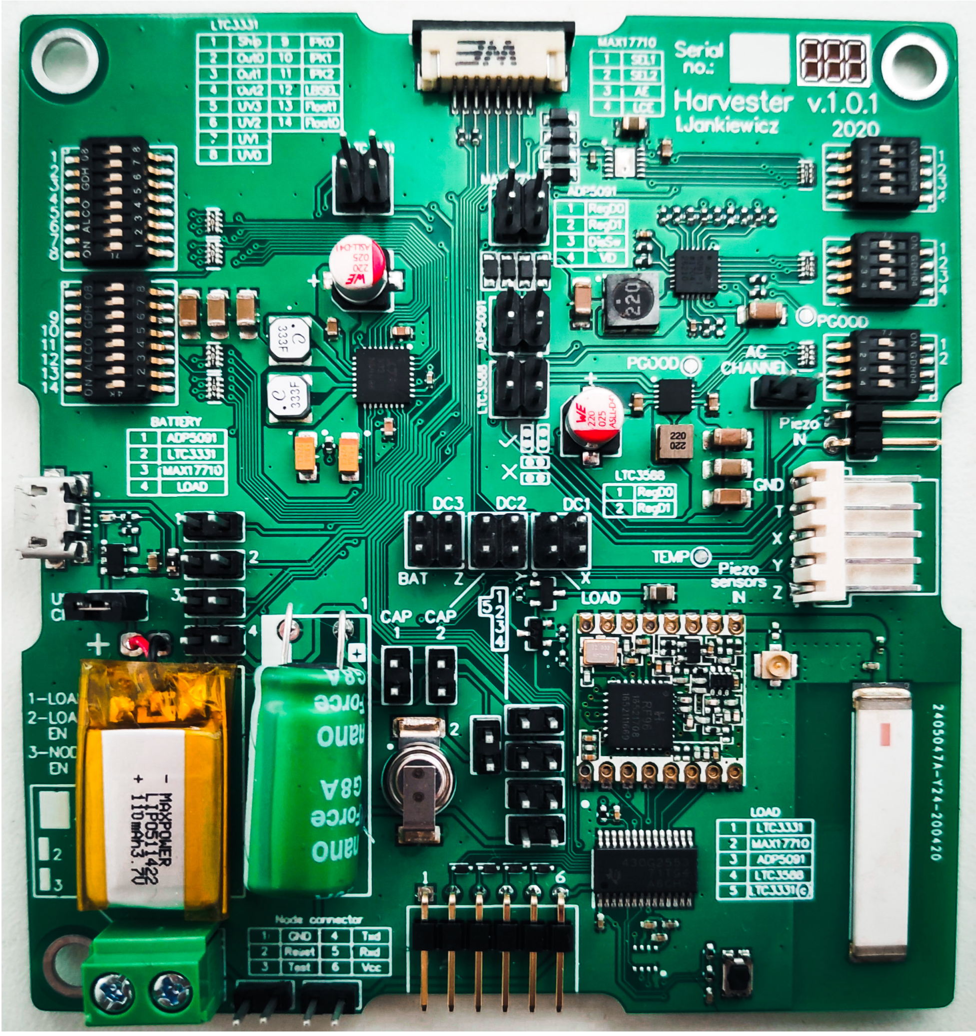

Figure 5.2: Assembled Harvester board

5.2 *Board testing*

The testing process consists of a few steps. The first one is to control all voltage rails to verify their performance. Subsequently, the reference voltage source has been checked. The next step is to validate relay operation, button and switches operation as well as LED indicators.

Providing that all previously mentioned tests were successful, it is time to connect the logger board to the PC and check its response for all commands. In the same time, the firmware also gets through the verification process. All input channels were tested using signal generator. The testing procedure involved applying sine signal of frequency from 1Hz to 1kHz in order to verify analog front-end operation and the sampling rate.

By increasing the testing signal frequency, the response of the anti-aliasing filter has been checked. Since all above-mentioned tests were successful, it is time to calibrate the logger board.

5.3 *Calibration*

Calibration is the last step required to finish the design of the logger board.

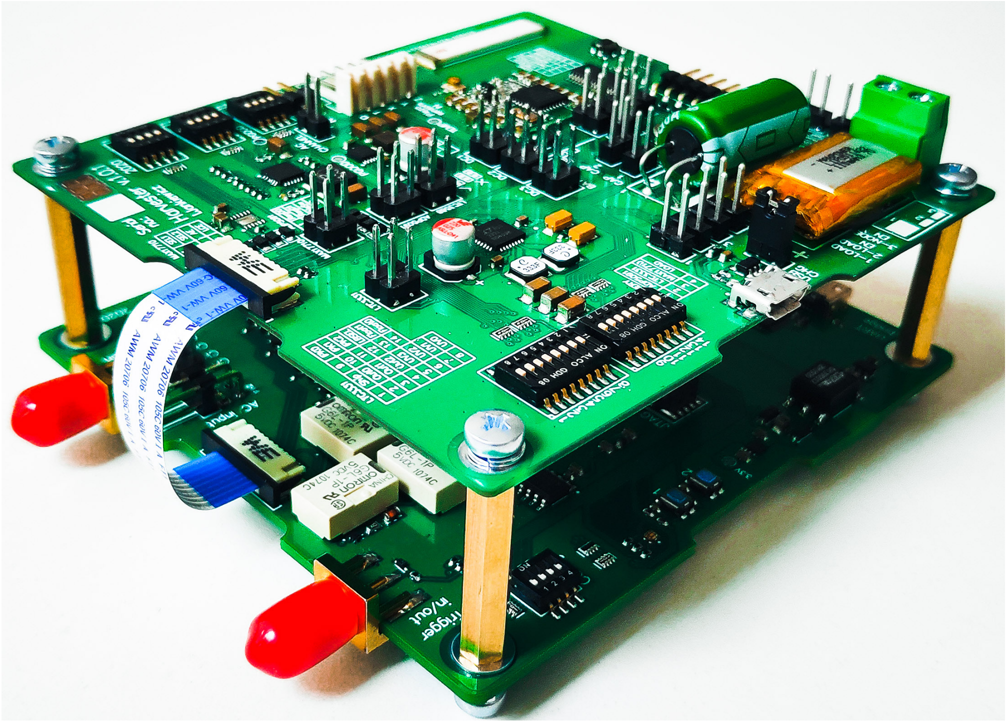

Figure 5.3: Assembled set of PCBs

6 LABORATORY TESTS AND RESULT ANALYSIS

The following section describes the procedure of evaluation of designed devices. The aim of the measurement setup is to recreate vibration events in real life, therefore allowing to verify usefulness of piezoelectric energy harvesters.

6.1 The measurement setup

In order to create appropriate testing conditions, it is necessary to come up with some kind of vibration generator. Owing to the fact that it is impossible to make use of a proper device designed for this purpose, another solution is to be provided.

The proposed solution is presented in the Figure 6.1. The piezoelectric beam is mounted in previously described holder. The mentioned holder is then attached to a long DIN rail that would be used to transfer the vibration. The DIN rail has to be properly mounted, therefore a vice is used to stabilize it in one position. Vibrations would be generated by hitting the rail with a piece of wood. Force direction is indicated in the picture.

The accelerometer board attached to the piezo holder is providing the actual acceleration value. Along with this signal, there is also a connection between the piezoelectric beam and the harvester board. Optionally, it is possible to monitor the temperature.

The harvester board is connected to the logger board using a ribbon cable. The logger board is used to monitor the accelerometer readings and the output of particular converters. It could be configured differently, but in case of all performed tests, this configuration is not a subject of change. The logger board is connected to the personal computer gathering all the samples. The load connected to the converter is a decade resistor that would allow to alter the load value during measurements.

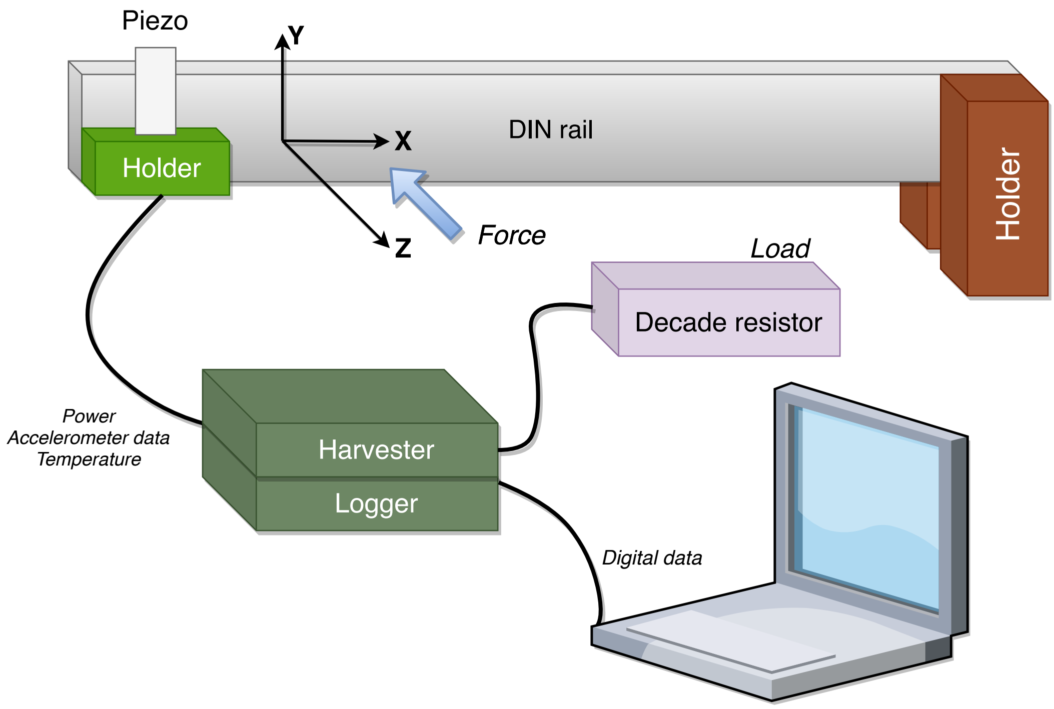

Figure 6.1: A diagram of measurement setup

6.2 Assumptions

On the beginning of data analysis it is vital to provide some assumptions related to the operating conditions of the harvester. The section regarding the building blocks of particular energy harvesters explained the structure of these devices and shown that they usually consist of input section based on storage components (capacitors) and the output stage which is a BUCK or BOOST converter. While it is possible to regulate the load connected to particular converters, the major impact on performance of the entire harvester is the impedance of the DC converter at its input. Due to the fact that the mentioned impedance is non-linear and mostly influenced by the behaviour of the input capacitance of the DC converter, the impedance matching is difficult to implement.

During all of performed measurements, it is assumed that the input capacitance of the converter was pre-charged, as it was possible to supply the load with some current just after one excitation of the rail attached to the piezoelectric harvester. Again, it should be noted that the measurement setup does not allow to provide repetitive testitng conditions, since the excitation of the rail was performed by human arm. Nevertheless, the following sets of measurements gave similar results.

6.3 Analysis of captured data

The exemplary data received during experiments is presented in the Figure 6.2. There are three different characteristics presented, namely the output voltage of the DC converter, the output current and the output power. All these curves are combined with accelerometer readings. The chonverter used in the example is the *LTC3588-1* connected to resistive load of 5kΩ.

The logger board is able to monitor both accelerometer output and the DC converter output. Owing to the fact that the load resistance of the DC converter is known, it is possible to calculate the current and output power generated by the harvester. Please note that the output voltage of the converter was set to 3.0V, but it did not reach stable level, because the energy generated by the piezoelectric beam was not sufficient.

Power generation of the energy harvester is mostly dependent on the input capacitor of the DC converter. Owing to the fact that

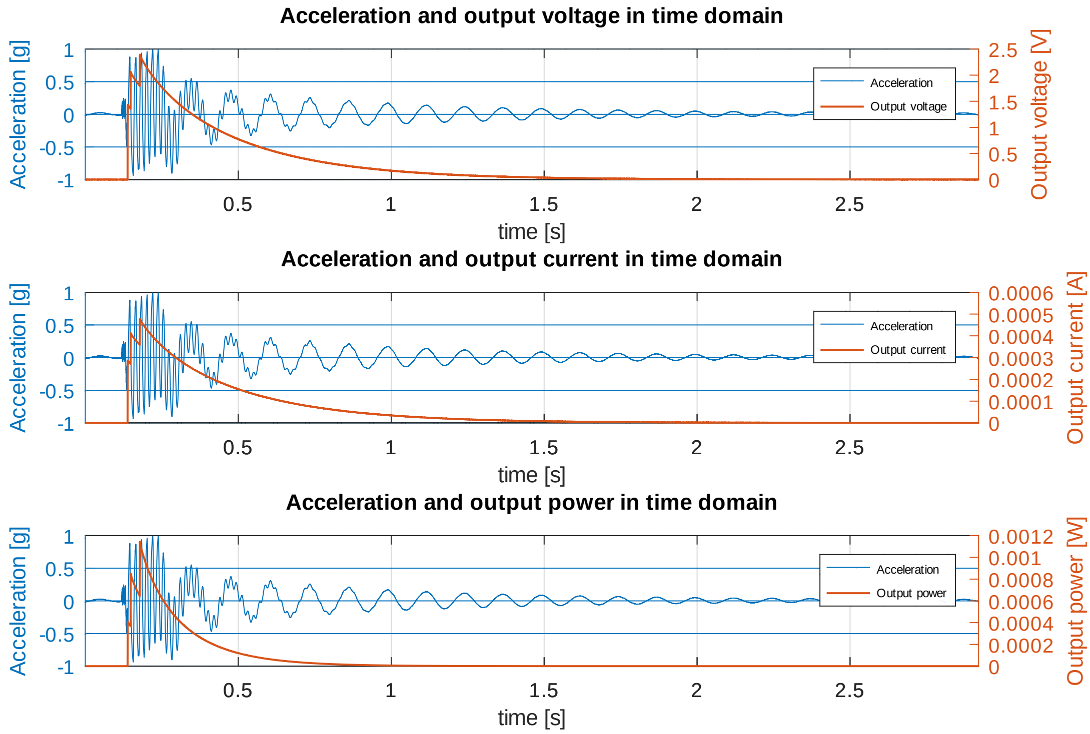

Figure 6.2: Measurement results example. Converter: *LTC3588-1*, Load: 5kΩ.

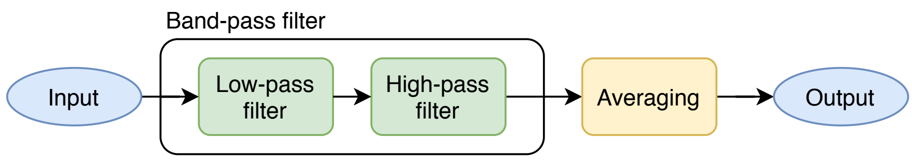

Figure 6.3: Accelerometer data conditioning

REFERENCES

1. Stephen Beeby, N. W. *Energy Harvesting for Autonomous Systems* ISBN: 978-1-59693-718-5 (Artech House, 2010).
2. Alper Erturk, D. J. I. *Piezoelectric Energy Harvesting* ISBN: 978-0-470-68254-8 (John Wiley & Sons, Ltd, 2011).
3. Tian, C. Energy harvesting from low frequency applications using piezoelectric, materials (Jan. 2019).
4. Thorsten Hehn, Y. M. *CMOS Circuits for Piezoelectric Energy Harvesters* ISBN: 978-94-017-9288-2 (Springer Science+Business Media Dordrecht, 2015).
5. Shuxiang JieFang Li, D. V. Theory Analysis on Magnetoelectric Voltage Coefficients of theTerfoneol-D/PZT Composite Transducer (June 2003).
6. *PPA Products. Datasheet and User Manual* PPA-1001. Revision No. 002. Midé Technology (2016).
7. Louis E. Frenzel, J. *Electronics Explained* ISBN: 978-1-85617-700-9 (Newnes (Elsevier Inc.), 2010).
8. *AN4508 Application note. Parameters and calibration of a low-g 3-axis accelerometer.* Revision No. 001. STMicroelectronics group (2014).
9. *ADXL335 datasheet* Revision No. 000. Analog Devices Inc. (2009).
10. *BRCL4054CME datasheet* Revision B. Foshan Blue Rocket Electronics (2018).
11. *AP2112 datasheet. Documnet number: DS39724* Revision no.2-2. Diodes Incorporated (June 2017).
12. *MCP9700 datasheet* Revision F. Microchip Technology Inc. (July 2017).
13. Burton, D. Op Amp Input Overvoltage Protection: Clamping vs. Integrated (May 2016).
14. Willams, T. *Circuit Designer'S Companion* ISBN: 978-0750617567 (Newnes (An imprint of Butterworth-Heinemann), 1993).
15. *BAS40-02V-V-G datasheet* Revision 1.1. Vishay Semiconductors (May 2012).
16. *OPAx180 datasheet* SBOS584E. Texas Instruments (Jun 2018).
17. Kester, W. *Mixed-Signal Hardware and Housekeeping Techniques* (Analog Devices Inc., 2006).
18. *Precision Thin Film Nichrome Chip Resistors* TT Electrinics (July 19).
19. *INA159 datasheet* SBOS443. Texas Instruments (Nov 2008).
20. *NTJD5121NT1G datasheet* Rev. 9. ON Semiconductor (May 2019).
21. Baker, B. C. *Designing an anti-aliasing filter for ADCs in the frequency domain* (Texas Instruments, 2015).
22. *RF50xx datasheet* SBOS410I. Texas Instruments (Jan 2020).
23. *MSP432P401R datasheet* SLAS826H. Texas Instruments (June 2019).
24. *Precision ADC With 16-Bit Performance* SLAA821. Texas Instruments (Jan 2018).
25. *ADuM1200/ADuM1201 datasheet* Rev. K. Analog Devices (2016).
26. *MAX14851 datasheet* REV. 1. Maxim Integrated (July 2019).

27. *CP2102/9 datasheet* REV. 1.8. Silicon Labs (Jan 2017).
28. *CP2130 datasheet* REV. 0.7. Silicon Labs (Jan 2014).
29. *LTC3588-1 datasheet* REV. C. Linear Technology (2010).
30. *X5R Dielectric, 4 – 50 VDC (Commercial Grade) series datasheet* AVX (2009).
31. *865060442002 datasheet* REV. 1.0. Würth Elektronik (Nov 2014).
32. *74438335220 datasheet* REV. 1.003. Würth Elektronik (Oct 2019).
33. *LTC3331 datasheet* REV. C. Linear Technology (2014).
34. *LPS4012 datasheet* Document 433. Coilcraft (2014).
35. *TAJ series datasheet* AVX (2010).
36. *ADP5091/ADP5092 datasheet* REV. A. Analog Devices (2017).
37. *744042220 datasheet* REV. 6.4. Würth Elektronik (Jan 2015).
38. *PMEGxx05EH/EJ series datasheet* REV. 02. Nexperia (Jan 2010).
39. *MAX17710 datasheet* REV. 2. Maxim Integrated (Dec 12).
40. *885012105002 datasheet* REV. 1.0. Würth Elektronik (Nov 14).
41. *885012106012 datasheet* REV. 1.0. Würth Elektronik (Nov 14).
42. Cartwright, K. V. Non-Calculus Derivation of the Maximum Power Transfer Theorem (2008).
43. *LiPo 511422 datasheet* Maxpower Industrial Co., Ltd. ().
44. *DRL series datasheet* Samxon ().
45. *Electric Double Layer Capacitor "DYNACAP" DS,DSK datasheet* Elna (2004).